(12)

Study of Chemiluminescent Reactions of Metal Atoms

Prepared by

J. F. Friichtenicht, Principal Investigator

S. P. Tang and Brian G. Wicke

TRW Defense and Space Systems Group

One Space Park
Redondo Beach, California 90278

November 28, 1977

Final Report

Prepared for

Naval Research Laboratory

Washington, D.C.

SECURITY CLASSIFICATION OF THIS PAGE *(When Data Entered)*

REPORT DOCUMENTATION PAGE

READ INSTRUCTIONS BEFORE COMPLETING FORM

1. REPORT NUMBER

2. GOVT ACCESSION NO.

3. RECIPIENT'S CATALOG NUMBER

4. TITLE *(and Subtitle)*

STUDY OF CHEMILUMINESCENT REACTIONS OF METAL ATOMS.

5. TYPE OF REPORT & PERIOD COVERED

Final Technical rept.
28 Jul 76 - 28 Nov 77.

6. PERFORMING ORG. REPORT NUMBER

7. AUTHOR(s)

Joseph F. Friichtenicht, Principal Investigator
S. P. Tang
Brian G. Wicke

8. CONTRACT OR GRANT NUMBER(s)

N00173-76-C-0258,
w/ DARPA Order-2062

9. PERFORMING ORGANIZATION NAME AND ADDRESS

TRW DSSG
One Space Park
Redondo Beach, California 90278

10. PROGRAM ELEMENT, PROJECT, TASK AREA & WORK UNIT NUMBERS

DARPA 2062 - Ammendment II

11. CONTROLLING OFFICE NAME AND ADDRESS

Naval Research Laboratory
4555 Overlook Ave. S.W.
Washington, D. C. 20375

12. REPORT DATE

28 November 1977

13. NUMBER OF PAGES

73

14. MONITORING AGENCY NAME & ADDRESS *(if different from Controlling Office)*

81p.

15. SECURITY CLASS. *(of this report)*

Unclassified

15a. DECLASSIFICATION/DOWNGRADING SCHEDULE

16. DISTRIBUTION STATEMENT *(of this Report)*

Approved for public release; distribution unlimited.

17. DISTRIBUTION STATEMENT *(of the abstract entered in Block 20, if different from Report)*

18. SUPPLEMENTARY NOTES

19. KEY WORDS *(Continue on reverse side if necessary and identify by block number)*

Chemiluminescence
Chemical Laser
Molecular Beam
Lifetime
Laser Vaporization

20. ABSTRACT *(Continue on reverse side if necessary and identify by block number)*

Laser vaporization of thin metal films has been used as the metal atom beam source for the study of chemiluminescent oxidation reactions. Techniques have been developed and demonstrated to experimentally determine the chemiluminescent reaction stoichiometry, the relative chemiluminescent cross section vs. kinetic energy, the total scattering cross section vs. kinetic energy, the total reactive cross section (under favorable conditions), the chemiluminescent spectrum and radiative lifetimes of chemiexcited species with

DD FORM 1 JAN 73 1473 EDITION OF 1 NOV 65 IS OBSOLETE

unclassified
SECURITY CLASSIFICATION OF THIS PAGE *(When Data Entered)*

lifetimes in the approximate range 10-100 μsec. The versatility of the laser vaporization metal beam source has been demonstrated by obtaining the chemiluminescent spectra for the N_2O oxidation of twenty different metal atoms under essentially identical experimental conditions. A definitive measurement of a long lived chemiexcited state has been made for the Pb + N_2O reaction; screening tests on Sn, Mo, and Ge oxidation by N_2O suggest these reactions also produce long lived excited states.

ABSTRACT

Laser vaporization of thin metal films has been used as the metal atom beam source for the study of chemiluminescent oxidation reactions. Techniques have been developed and demonstrated to experimentally determine the chemiluminescent reaction stoichoimetry, the relative chemiluminescent cross section vs. kinetic energy, the total scattering cross section vs. kinetic energy, the total reactive cross section (under favorable conditions), the chemiluminescent spectrum and radiative lifetimes of chemiexcited species with lifetimes in the approximate range 10-100 μsec. The versatility of the laser vaporization metal beam source has been demonstrated by obtaining the chemiluminescent spectra for the N_2O oxidation of twenty different metal atoms under essentially identical experimental conditions. A definitive measurement of a long lived chemiexcited state has been made for the Pb + N_2O reaction; screening tests on Sn, Mo, and Ge oxidation by N_2O suggest these reactions also produce long lived excited states.

TABLE OF CONTENTS

LIST OF FIGURES

LIST OF TABLES

1. INTRODUCTION

The purpose of this program was to develop experimental techniques for the study of metal oxidation chemiluminescent reactions, and to utilize these techniques to obtain chemical kinetic data on these reactions. In connection with development of a visible wavelength chemical laser, particular emphasis was placed on obtaining chemiluminescent spectra and measuring radiative lifetimes of appropriately long lived chemiexcited metal oxidation products.

Key to this experimental program was the use of the TRW developed laser vaporization metal atom source. Use of this versatile source has allowed the study of the oxidation kinetics of a wide variety of different metal atoms under essentially identical experimental conditions. Great care has been exercised to fully document and test all procedures in order to insure reliability of the techniques and results.

Section 2 of this report describes the apparatus we have used in studying chemiluminescent oxidation reactions of metal atoms. Experimental procedures and data reduction techniques developed for this work are described in detail in Section 3. Section 4 presents the experimental results obtained during this program. Section 5 contains a brief summary. Technical papers and presentations resulting from this work appear in the appendices.

2. EXPERIMENTAL APPARATUS

All our experiments have been performed in a molecular beam environment (although not always under single collision conditions). A pulse of metal atoms is produced by laser vaporization of a thin metal film (Section 2.1). This metal atom beam then interacts with an oxidant gas at a known low pressure in a special region of the beam apparatus. Diagnostic data are obtained by monitoring the attenuated and unattenuated metal atom fluxes, by monitoring chemiluminescent intensity and spectral distribution, and by monitoring the time decay of chemiexcited reaction products to obtain information on the radiative lifetimes of these products.

A schematic diagram of the molecular beam apparatus is shown in Figure 1. The essential features of this apparatus are described separately below.

2.1 LASER VAPORIZATION SOURCE

The unique feature of our experimental approach is the use of laser vaporization of thin metal films as the metal atom beam source. This technique[1] was first proposed and demonstrated by J.F. Friichtenicht at TRW. Stated most simply, the rapid deposition of energy from a Q-switched laser on an opaque metal target is used to heat the metal and cause significant vaporization.

The metal of interest is vacuum deposited as a thin film (nominally one micron) on a transparent substrate (typically a microscope slide). Such vapor deposition of a wide variety of metals is a simple procedure for a suitably equipped laboratory and is performed routinely for us by a solid state group within TRW. Purity of the metal target (and hence the beam) is limited by that of the metal sample used in vapor deposition. The target so prepared is then transferred to the source chamber of the beam facility; standard vacuum locks are used to insert the metal sample. Inside the high vacuum chamber, the metal film is irradiated <u>through the transparent substrate</u> by a Q-switched ruby laser. Typically a one joule laser pulse of 80 nanosecond duration irradiates a spot of 2mm diameter. An intense plasma of metal atoms, ions, and free electrons is created

CHEMILUMINESCENCE MEASUREMENT CONFIGURATION

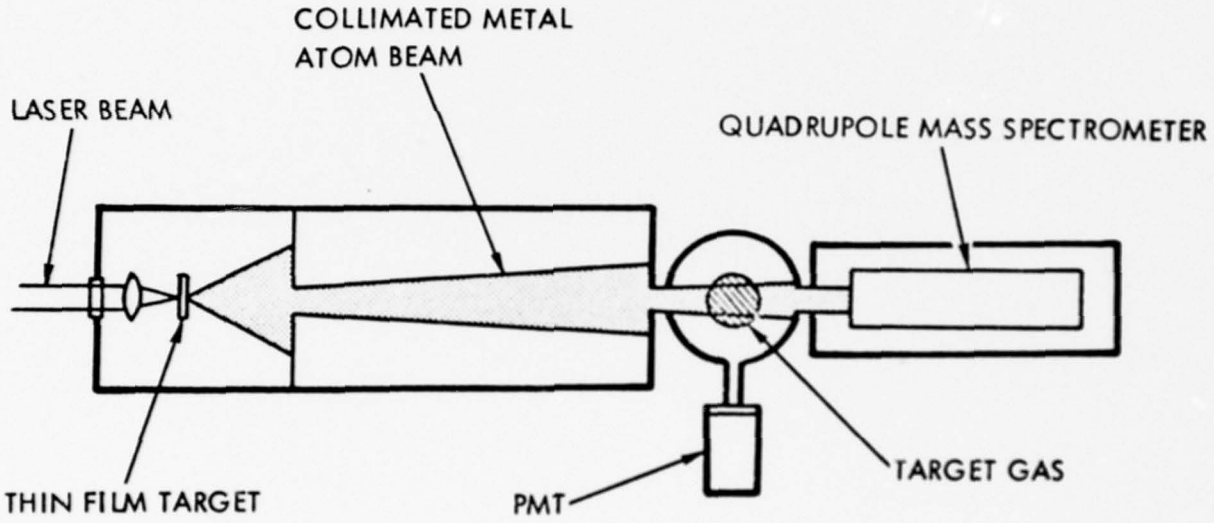

Figure 1. Schematic diagram of the atomic beam apparatus used to study chemiluminescent metal atom oxidation kinetics.

TRW SYSTEMS GROUP

by this laser heating.[1] Because this hot, dense plasma is contained on one surface by the substrate and on the other surface by the remaining film, significant moderation of the temperature results before the film thickness is vaporized. By appropriate choice of laser energy density and film thickness, virtually all ions created in the initial plasma have recombined before the film is consumed. The resulting dense metal vapor cloud expands and becomes collisionless within several cm (see below) of the substrate. The expanding vapor is then collimated and is ready for use as a pulsed source of metal atoms. Because the laser vaporization is nearly instantaneous (80 nsec) and the cloud becomes collisionless very near the substrate, the arrival time of a metal atom at a downstream position specifies the atom's velocity.

The metal atom pulse is quite intense. Nominally 10^{17} metal atoms are vaporized from the small spot.[1] The vapor cloud is approximately an expanding sphere, the center of mass of which is moving away from the substrate.[2] Hence, significant forward peaking occurs in the angular distribution. The time-integrated flux at a position 10 cm from the substrate is approximately 10^{15} atoms/cm^2, with kinetic energies ranging from 0.1 eV to approximately 10 eV. After producing one pulse, the target is moved to expose another spot for laser irradiation. The repetition rate is limited to one shot per minute by thermal characteristics of our ruby laser system.

Because of this pulsed nature of the beam source, pulsed detection is required. One advantage of this pulsed beam source is the kinetic energy information available.[1,3] Such kinetic energy data are usually very difficult to obtain using conventional metal beam sources, requiring chopping techniques or seeded nozzle beam methods. The most significant advantage of this laser vaporization source, however, is the wide variety of metal atoms which can be studied with essentially the same apparatus. Table 1 documents this versatility for neutral atomic beams. Metal atoms studied in this program are designated by a "*" in the table.

The thin film targets in column 1 were prepared early in the contract (or prior to the contract) and were readily available during the experimental work. Metals in column 3 of this table are reactive with air and

Table 1. Metal Atom Thin Film Targets
(Ordered by Atomic Number)

Targets Currently Available		Targets Being Prepared	Targets Requiring Special Handling
*B	*Mo	Sc	Li
C	*In	V	Be
*Al	*Sn	Cu	Na
*Si	*La	Zn	*Mg
*Ti	Ce	Y	K
*Cr	*Nd	Cd	Ca
*Mn	*Sm		Rb
*Fe	*Ho		Sr
*Co	*Au		Ba
*Ni	*Pb		
*Ge	U		

* Indicates metals studied in this program.

consequently require special handling and storage between preparation and use. Because of lack of time, the only metal targets in the third column that were made were magnesium and barium. The barium targets were air oxidized during a handling error and could not be used.

Reduced metal fluxes and photon signals were observed for numerous metals near the end of this program. Many of the metal targets were a year old by this time. It is not surprising that even for relatively unreactive metals thin film samples oxidize significantly over an extended period. Indeed, metal oxides were observed using the quadrupole mass spectrometer for several metals in the absence of any oxidant in the interaction region, suggesting oxidation of the target itself. In the future targets will be used shortly after being prepared or will be stored under vacuum.

The specific characteristics of the metal pulse formed by laser vaporization depend on the metal, the film thickness and the laser energy density.[1,2] (Laser pulse duration is doubtless a factor as well, but was not adjusted in this work.) Experiments were conducted to examine the dependence of the metal flux on these parameters to insure that the maximum metal flux was obtained consistent with good beam characteristics, particularly a smooth velocity distribution, absence of ions, and shot-to-shot reproducibility. Laser energy density was varied using constant flashlamp energy and varying the irradiated spot size on the target using an externally movable lens. (It was separately verified that changing the laser energy with constant spot size gave the same qualitative changes in the metal atom flux characteristics.)

Metal film thickness tests on several metals showed that one micron thickness was a good compromise for the current system, allowing relatively large metal fluxes with approximately 2mm diameter spot size.

Numerous difficulties with the ruby laser system were encountered during the program, accounting for an appreciable part of the unexpected delays. At least part of our laser difficulties doubtless arose from operating near the high power output limit. Changing to a neodymium laser would significantly increase the available laser energy and correspondingly allow reduction in the operating conditions; a neodymium laser is under construction.

The transition from a very dense metal vapor cloud near the target to a collisionless metal atom beam occurs within a few cm of the target.[1,2] It is essential in our experiments that the interaction region be far enough from the target to insure a collisionless beam. In order to insure adequate but not excessive separation, experiments were performed examining the metal atom flux and pulse characteristics as a function of distance from the source target to the interaction region. These experiments as well as careful examination of metal deposit shadow patterns formed on the apparatus walls established that the metal vapor cloud was essentially collisionless within less than 5 cm of the target. This result was used in designing the special apparatus for measuring chemiluminescent spectra; the increased metal flux resulting from this optimized design contributed significantly to our ability to measure some of the weaker chemiluminescent spectra.

2.2 INTERACTION REGION

Once the pulse of metal atoms is formed and collimated, a conventional beam apparatus is used with the exception that time dependent detection is employed. Metal atom collisions with various oxidants are studied in a differentially pumped interaction region located downstream from the metal target (see Figure 1).

In the experiments performed on this contract, we have utilized the so-called beam-gas configuration. The interaction region consists of a small chamber with entrance and exit channels for the incident metal atom beam and the molecular products. Oxidant pressure is measured by an absolute, single sided capacitance manometer. Hence, the probability that a metal atom will react with the oxidant depends on known parameters (oxidant number density and effective path length) and the interaction cross section (to be determined by the experiment).

2.3 UNIVERSAL DETECTOR

A universal detector (composed of an electron impact ionizer, electrostatic ion extraction optics, a quadrupole mass spectrometer, and an electron multiplier) is located downstream from the interaction region on the axis defined by the incident metal atom beam.[3] This detector has been used almost exclusively as a metal atom monitor, although metal oxide

products were sometimes examined as well. Our primary interest has been in chemiexcited products which were detected by the photons they emit (see Section 2.4).

No attempt was made to make quantitative corrections to compare the fluxes of different metal atoms observed by the quadrupole mass spectrometer (QMS). There are generally accepted techniques[4] for accounting for differing ionizing efficiencies and mass dependent transmission effects, and in future experiments such corrections should be examined. For a given metal, however, considerable effort was expended to insure that the observed QMS signal vs time was a good measure of the relative metal number density vs time; that is, to insure that the transmission of the QMS was not a sensitive function of atom kinetic energy. Several calibration experiments were considered to demonstrate this, but none was thought to be conclusive. Instead, a detailed empirical survey was made of the effects of various adjustments of the ionizer, extraction lenses and the quadrupole on the observed metal atom pulse shape. It was found that at high QMS resolution settings, spiked and irregular metal atom pulse shapes were obtained, probably resulting from the very narrow kinetic energies passed by the quadrupole at high resolution. As the resolution was reduced, however, a smooth time-of-flight distribution was obtained. Further reduction in QMS resolution did not alter the shape of the distribution, but merely increased its overall intensity (as more trajectories were passed by the spectrometer). Similar results were obtained by modifying the ionizer controls; namely, as focusing conditions were relaxed, a smooth time-of-flight distribution was obtained which upon further reduction in the conditions did not change in a qualitative way. We believe that this general shape obtained by relaxing focusing and resolution conditions of the QMS system accurately represents the true time-of-flight distribution of the metal pulse. This general time-of-flight distribution is also in good agreement with that predicted by a theoretical model describing laser vaporization.[2] For relaxed electrostatic focusing and quadrupole resolution conditions, it is not surprising that the observed time-of-flight distribution is an accurate reflection of the true distribution, since the ion focusing potentials and the ultimate ion kinetic energy are significantly greater than the initial metal atom kinetic energy.

2.4 PHOTON DETECTION

Photon detection is accomplished using bare and filtered photomultipliers, and a Princeton Applied Research optical multichannel analyzer (OMA). The phototubes used were two Centronics 4282B's and one Centronics 4282R (high efficiency bialkali photocathode), an RCA 8575 (bialkali photocathode with 116 response), and an RCA 31034 (GaAs photocathode with a 128 response). Each tube was calibrated as a function of wavelength, and the absolute gain was established as a function of multiplier voltage.

Chemiluminescent spectral data were obtained using the optical multichannel analyzer. Briefly, the OMA system is composed of a converted .25 meter monochromator and an array of 500 detectors, each .5 inches tall by one mil wide. The exit slit of the monochromator is removed, converting it to a polychromator. The detector array is placed in the polychromator image plane, with each of the 500 detector elements monitoring a narrow wavelength window of the dispersed light. In essence the system is very similar to use of a photographic plate in the exit plane of a monochromator, except that the OMA response is linear in the number of photons (see Section 3.3, however) and the "developing" is accomplished by electronic readout and semiconductor memory storage. Our converted monochromator has several gratings, allowing simultaneous measurement of a 200 nm wide spectrum (with up to 0.4 nm resolution) or a 50 nm wide spectrum (with up to 0.1 nm resolution).

Our OMA includes several factory modifications to enhance its capability. A silicon intensifier stage improves the quantum efficiency markedly, although it does introduce an S-20 wavelength response characteristic. With the intensifier, the OMA has a sensitivity of approximately one count per 12 photons (at 450 nm). A scintillator has also been added to improve the ultraviolet response. The detector may be cooled to dry ice temperatures, allowing data storage on the vidicon itself for up to several hours. In order to utilize this storage capability, we also have an extended delay unit for the OMA. This OMA system is expensive, and was purchased for use in our laboratory with TRW capital funds.

This commercial optical multichannel analyzer is a very sophisticated device. Perhaps naively, we significantly underestimated the complexity

of operating this device for low light levels, and had considerable growing pains while we learned its intricacies. Subtleties associated with preconditioning the surface for signal accumulation and optimal readout of low light level signals are illusive, at the very least. It required several months of serious effort to obtain reliable spectra from low level signals. In retrospect, little of this learning time could have been significantly reduced or eliminated, given the initial information available from the manuals. This learning experience was well worth the effort; with the OMA we have been able to obtain the chemiluminescent spectra for twenty different metal atom oxidation reactions (see Section 4.3).

2.5 LIFETIME APPARATUS

An important part of our experimental investigation involves measurement of the radiative lifetimes of chemiexcited species if these lifetimes are in the approximate range 10-100 μsec. Our lifetime apparatus is shown in Figure 2. The essential features of our time-of-flight lifetime technique may be understood as follows.

A pulse of metal atoms is formed by laser vaporization of a thin film, as usual. A rotating chopper, synchronized with the Q-switch of the ruby laser, allows a narrow velocity slug of the metal beam to enter the interaction region, where it may interact with oxidant. Because the metal atom is typically much heavier than the oxidant, and because the metal atom is traveling with considerable kinetic energy before a reactive collision, the metal oxidation product is predominantly forward scattered in the laboratory coordinate system. (The degree of forward peaking in the laboratory coordinates obviously depends on the identity of the metal atom and oxidant, the initial kinetic energies, and the reaction exothermicity.) Some of the metal oxidation products therefore travel through the interaction region exit port and into the differentially pumped lifetime chamber (see Figure 2). If these product molecules are electronically excited but have radiative lifetimes long enough (tens of microseconds) to live until they drift into the lifetime chamber, their presence may be detected by their photon emission in this chamber. Because the pressure in the lifetime chamber is kept very low, there are few collisions in this chamber, and the product molecule velocity is unchanged during its flight through this lifetime chamber. Hence the photon signals observed at the

RADIATIVE LIFETIME MEASUREMENTS CONFIGURATION

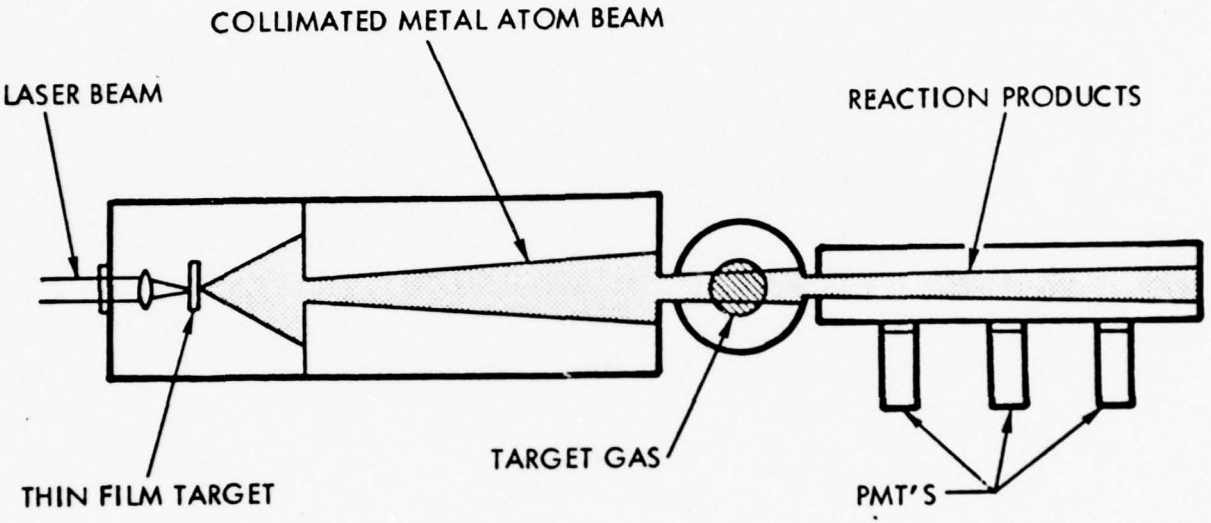

Figure 2. Schematic diagram of the atomic beam apparatus used to study long-lived chemiexcited metal oxidation products.

TRW SYSTEMS GROUP

lifetime chamber ports as a function of time contain information on the product molecule kinetic energy and the lifetime of the species doing the radiating. In an *idealized* experiment these long lived reaction products would be detected as an exponentially decreasing signal at the three observation ports.

Considerably more will be said about this technique and the associated data reduction procedures in Section 3.4.1.

3.0 DATA ACQUISITION AND ANALYSIS PROCEDURES

In this section we describe in detail the methods used to obtain experimental data and the analysis techniques used in processing these data. Considerable time has been devoted to developing these various techniques, and to thoroughly validating their accuracy. In the case of the lifetime experiments, data analysis appeared at first to be straightforward but proved in fact to be more complicated.

3.1 CHEMILUMINESCENT REACTION STOICHIOMETRY

The most fundamental piece of chemical information to obtain about a chemiluminescent reaction is the stoichiometric dependence of the reaction -- that is, for the reaction of the general metal atom M with a general oxidant molecule Ox,

$$aM + bOx \rightarrow \text{products} + h\nu$$

what are a and b? (The identity of the products is obtained from the chemiluminescent spectra, Section 3.3.) This chemiluminescent reaction stoichiometry is determined experimentally be monitoring the chemiluminescent intensity in the interaction region (at a specific wavelength if desired) as a function of oxidant pressure and metal atom flux. The oxidant pressure is changed and monitored straightforwardly. The metal atom flux at a given kinetic energy (Section 3.2.1) is changed most simply by changing the target orientation relative to the laser;[1,2] this metal atom flux is monitored by the quadrupole mass spectrometer (see Figure 1). Chemiluminescent reaction stoichiometry may be obtained as a function of emission wavelength (excited state identity) and kinetic energy if desired.

3.2.1 Relative Chemiluminescent Cross Section

The typical chemiluminescent cross section experiment is performed using the apparatus shown in Figure 1. A pulse of metal atoms is produced by laser vaporization of an appropriate thin film target. This metal vapor pulse travels down the apparatus to the interaction region, where some of the metal atoms react. For sufficiently low oxidant pressure,

most of the metal atoms travel through the interaction region and are detected by the QMS. In the interaction region, any chemiexcited product molecules which emit photons are detected using a phototube mounted on the interaction region.

Both the chemiluminescent signal from the interaction region and the QMS signal are obtained as functions of time. The system background pressure is low enough that no collisions with background gas occur, and the oxidant pressure in the interaction region is adjusted to be small enough that most of the metal atoms (95%) do not undergo any interaction with this oxidant. Because most metal atoms travel through the apparatus without undergoing any interactions, their times of arrival (relative to the firing of the laser) at a position downstream from the metal target are determined by the distance from the target to the detector (ℓ) and the atoms' velocities, v,

$$t(\text{arrival}) = \ell/v$$

Hence the various diagnostic signals vs time can be converted into signals vs kinetic energy of the atom. For the phototube on the interaction region, the signal gives the rate of formation of excited products as a function of metal atom velocity. For the QMS, the signal gives the number density of the metal atoms in the ionizer as a function of metal atom velocity. (In obtaining the relative atom number density vs velocity from the QMS signal, corrections are made for the ion transit times from the ionizer through the quadrupole and to the detector.) This metal atom number density at the ionizer vs velocity can be converted to metal flux at the ionizer vs velocity, which in turn can be converted to metal flux at the interaction region vs velocity. It is essential for these considerations that the oxidant pressure in the interaction region be kept low enough that most metal atoms are not scattered significantly, for two reasons; (1) if appreciable scattering occurs in the interaction region, the flux observed at the QMS will not accurately reflect the incident flux at the interaction region, and (2) if appreciable scattering occurs in the interaction region, some metal atoms reach the QMS having had one velocity from the target tothe interaction region, and another velocity from the interaction region to the QMS. In our experiments the total

attenuation of the metal atom beam from all sources can be monitored (using the QMS) as oxidant is added to the interaction region; chemiluminescent cross section data are taken only when the metal atom attenuation is less than 5% for any velocity observed.

The rate of formation of chemiexcited product molecules in the interaction region is proportional to the product of the incident metal atom flux, the oxidant number density, and the chemiluminescent cross section. The oxidant number density is known from the pressure in the interaction region (as measured by a capacitance manometer) and the (relative) incident metal atom flux is known from the corrected QMS signal. Hence the chemiluminescent cross section vs kinetic energy can be obtained from the observed chemiluminescent intensity vs atom kinetic energy.

As mentioned previously, no attempt has as yet been made to correct the QMS signals for differences in ionization efficiencies and mass dependent transmission effects. As a result, the chemiluminescent cross sections obtained here are relative measurements.

3.2.2 Total Scattering Cross Section

The total scattering cross section for a metal atom interacting with a particular oxidant is obtained by monitoring the metal atom flux at the QMS vs oxidant pressure in the interaction region. The entrance to the electron impact ionizer subtends an angle of 0.4° from the center of the interaction region, so that any scattering event in the interaction chamber which either completely removes the metal atom from the beam (e.g., a chemical reaction) or scatters the metal atom sufficiently to cause it to miss the ionizer aperture is included in this total scattering cross section.

The metal atom intensity I(v) at a particular velocity observed at the QMS is given by

$$I(v) = I(v)_0 \cdot \exp(-N' \cdot \ell \cdot \sigma_T(v)) \qquad (1)$$

where $I(v)_0$ is the incident metal atom flux in the absence of any scattering, N' is the number density of the scatterer in the interaction region, ℓ is the effective path length of the interaction region, and

$\sigma_T(v)$ is the total scattering cross section for this velocity. Because $I(v)$ and $I(v)_o$ cannot be measured simultaneously, care is used to insure reproducibility from shot to shot, and numerous shots are taken at each pressure to improve statistics. $I(v)$ vs v data at several pressures are obtained. A least squares' fit is then made to equation (1) for each kinetic energy, to obtain the total scattering cross section.

It should be noted that this is an absolute measurement, even though the absolute metal atom flux is still unknown. The magnitude of this cross section at a given kinetic energy puts an upper limit on the magnitude of the chemiluminescent cross section at this same kinetic energy.

3.2.3 Total Reactive Cross Section

It is possible to obtain an estimate of the total reactive cross section from chemiluminescent intensity vs oxidant pressure data, under favorable conditions, as follows. Consider an experimental arrangement as shown schematically in Figure 3. A well collimated beam of metal atoms enters the interaction region. Some known distance ℓ' away from this entrance, but still inside the interaction region, is a region of space which is viewed by a phototube. The observed volume is thin in the metal atom flow direction, but tall in both dimensions perpendicular to this flow. For short lived excited molecular products formed in this viewing region, the intensity of chemiluminescence observed by this photon detector is proportional to the rate of formation of chemiexcited products; for a reaction first order in the metal and first order in the oxidant, the observed chemiluminescent intensity is given by

$$I = C \cdot N' \cdot F_m \cdot \sigma_{chem} \qquad (2)$$

where C is a constant, N' is the oxidant number density, F_m is the metal flux entering the viewing volume, and σ_{chem} is the chemiluminescent cross section. (Note that the intensity, metal atom flux and cross section are not written as a function of velocity here. Time integrated quantities will be used.) The time integrated metal atom flux entering this viewing region may be expressed in terms of the integrated metal flux entering the interaction region F_{m_o} and the attenuation cross section σ' (see below) as

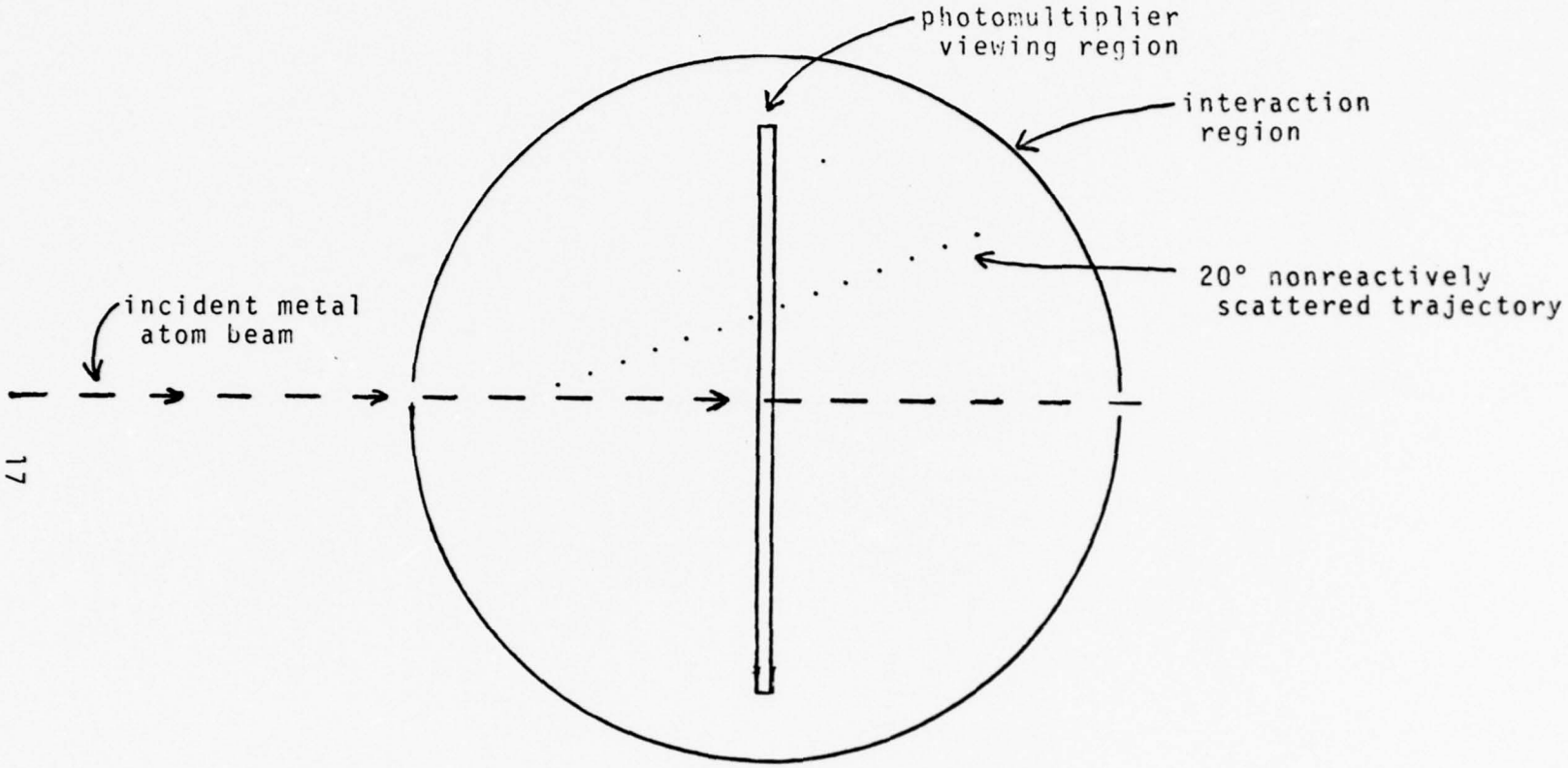

Figure 3. Schematic diagram showing geometry for estimating the total reactive cross section (see text).

$$F_m = F_{m_o} \cdot \exp(-N' \cdot \ell' \cdot \sigma') \qquad (3)$$

Combining equations (2) and (3), the observed chemiluminescent intensity from this thin viewing region is then

$$I = C \cdot N' \cdot \sigma_{chem} \cdot F_{m_o} \cdot \exp(-N' \cdot \ell' \cdot \sigma')$$

$$= C' \cdot N' \cdot \exp(-N' \cdot \ell' \cdot \sigma') \qquad (4)$$

(This expression applies for bimolecular chemiluminescent kinetics; analogous expressions for different chemiluminescent kinetics can be obtained.)

What processes contribute to σ'? Put a slightly different way, how can a metal atom which enters the interaction region fail to enter the viewing region? Obviously, if the metal atom reacts before reaching the viewing region, it is removed from consideration, so *all* reactive processes must be included in σ'. Suppose, however, a metal atom undergoes a nonreactive collision with an oxidant molecule. For a heavy metal moving with significant initial velocity (significant compared to the velocity of the oxidant molecule), a nonreactive collision with a light oxidant cannot scatter the metal atom by more than 10-20° in the laboratory coordinate system. (This maximum angle depends of course on the relative masses and initial kinetic energies.) Since the viewing geometry includes large deflections of the metal atom, this nonreactive collision should not be included in σ' above. Within these assumptions, then, the attenuation cross section σ' is composed of a sum of all reactive cross sections only. By measuring the time integrated chemiluminescent intensity vs oxidant pressure and fitting these data to Equation (4), the absolute total reactive cross section σ' can be obtained. It is important to note than an absolute cross section is obtained, just as in the case of the total scattering cross section (Section 3.2.2).

The above development ignores several problems. One potentially serious neglect is the possible velocity dependence of various reactive cross sections. Even if a nonreactive collision does not change the trajectory of a metal atom sufficiently to cause it to miss the viewing region, such a collision can slow the metal atom significantly. If any moderate energy threshold phenomena are present, this velocity change would very seriously compromise the analysis. Hence inherent in this analysis is the assumption that the velocity dependence can be ignored. Second, even though one nonreactive collision cannot remove a metal atom from trajectories passing through the interaction volume, *many* nonreactive collisions obviously could. Hence the cross section for wide angle nonreactive scattering must not be too much greater than the total reactive cross section for Equation(4) to be applicable. Finally, inherent in this development is the assumption that the pressure increase does not lead to secondary reactions.[5] If, for example, a metastable molecular product is formed during one collision, and then is quenched to another excited molecular product which does emit, the total intensity vs pressure data will not be adequately described by this model.

Under favorable conditions, then, this model is expected to give a reasonable estimate for the total reactive cross section. At low pressure the total chemiluminescent intensity is expected to follow a form characteristic of the reaction stoichiometry; a bimolecular reaction would show a linear increase in the intensity of chemiluminescence vs pressure. At higher pressures, attenuation of the metal atom beam will decrease this intensity, until finally the total intensity drops as a function of pressure. Serious deviations from this dependence indicate the inherent assumptions mentioned above are invalid.

3.3 CHEMILUMINESCENT SPECTRA

The most productive aspect of the data acquisition phase of this experimental program has been the measurement of the chemiluminescent spectra for various metal oxidation reactions. Using the cooled OMA in the time delay mode, the vidicon surface integrates light over an extended period of time. Even though the duty cycle for repetitive metal atom pulsing is poor -- namely, photons are produced in the interaction region for one hundred microseconds once every minute -- signal enhancement

from multiple shots in this delay mode is linear with the number of shots. (In fact, apparent enhancement is somewhat greater than linear. Weak signals are extremely difficult for the OMA vidicon scanning system to detect because of charging problems on the vidicon itself. Hence a signal corresponding to five counts is read with considerably less efficiency than one corresponding to then counts.)

Noise in the OMA spectrum results from four possible sources: (1) background photons; (2) dark current in the vidicon; (3) noise associated with electronic vidicon readout; and (4) quantum statistics. Background photons can be virtually eliminated from the system; experiments are performed in a darkened laboratory, and input optics are carefully baffled. Dark current (or leakage current) within the vidicon is a serious problem when operated at room temperature; in fact, the leakage current will cause the OMA to completely lose received signal in less than a second at room temperature. With the cooled detector, however, leakage is virtually eliminated; tests have shown that a signal received by the vidicon will remain virtually unchanged for several hours at dry ice temperatures. Vidicon readout noise and quantum statistics are the limiting sources of noise. For sensitivity approaching specifications, very special vidicon surface preconditioning and readout biasing are required, and under these conditions, readout noise is significant. It has been our experience that even after the fundamentals of the sensitivity enhanced OMA are appreciated, considerable experimentation is required to obtain uniform readout with high sensitivity and low noise.

Chemiluminescent spectral data are obtained by first performing survey spectra covering 200 nm regions in the visible with resolution of about 4 nm, and then more detailed spectra are obtained for interesting wavelength regions.

3.4 LIFETIME MEASUREMENTS

There is particular interest in measuring radiative lifetimes of chemiexcited species in the approximate range 10-100 μsec in connection with development of a visible wavelength chemical laser. We have developed a time-of-flight technique for measuring these lifetimes, as detailed below. Application of the detailed data analysis given in 3.4.1

requires moderately strong signals in the lifetime chamber with good statistics; furthermore, such measurements are time consuming. As an alternative screening procedure, we have developed a quicker though considerably less informative experimental procedure which is given in 3.4.2. The screening procedure is applied first, of course, to identify molecules worth the full scale testing. The full scale testing and model are described first, below, because many of the statements supporting the screening procedure derive directly from the detailed analysis.

3.4.1 Detailed Lifetime Analysis Technique

For the *idealized* experiment, as stated in Section 2.5, as the long lived chemiexcited product molecules travel through the lifetime chamber, they are decaying according to $\exp(-t/\tau)$, resulting in an exponentially decaying signal observed at the three spatially separated (and hence temporarily separated) observation ports. The observed intensity decay together with the observed arrival time differences are used to obtain the radiative lifetime. Unfortunately, this is an oversimplification.

The difficulty results essentially from two factors. First, most of the metal atoms entering the interaction region pass through without undergoing any interaction whatsoever; this is the case because the interaction region oxidant pressure is kept low to prevent excessive scattering of the product molecules. Most of the product molecules travel along the same axis as the incoming metal atom beam, as described in Section 2.5. As a result the molecular product and considerably more unreacted metal atoms enter the lifetime chamber. The second factor contributing to the complexity is that most diatomic molecules have long lived and short lived states which are energetically accessible in various oxidation experiments, particularly when the available kinetic energy is considered. Of course, a short lived molecular product formed in the interaction region is no problem in the lifetime chamber. However, there is inevitably some stray oxidant in the lifetime chamber. The unattenuated metal atoms entering the lifetime chamber may react with these stray oxidant molecules to produce short lived excited products directly in front of a detection port; these short lived excited species do contribute to the observed signal and can cause a significant deviation from the exponential intensity decay which is expected. It is this

contribution which causes the greatest confusion and was responsible for the anomolous preliminary results previously reported.[6]

Before proceeding with the model development, let us make clear that no other sources of photons observed in the lifetime chamber need be considered. We have already considered short lived and intermediate lived chemiexcited product molecules. Molecules with very long radiative lifetimes emit very slowly, so that an observed photon signal from such products in the lifetime chamber would be weak and constant from port to port ($\exp(-t/\tau) \simeq 1$). Though not expected to contribute significantly, it will be shown below that this constant contribution is accounted for by the model. No short lifetime excited metal atom will make it to the lifetime chamber. An intermediate lifetime excited metal atom might survive to emit in the lifetime chamber, but we check experimentally to be sure none is present. A metastable metal atom would not emit significantly in the lifetime chamber on its own; if such a long lived metastable metal collides with a molecule in the lifetime chamber and thereby produces a photon, this corresponds to the short lived reaction product case introduced above and to be treated below. These are the only sources of photons in the lifetime chamber; the only two sources of photons which must be considered are (1) intermediate lifetime chemiexcited molecular products produced in the interaction region which drift into the lifetime chamber (the desired photon signal) and (2) short lifetime excited molecular products *produced* immediately in front of the lifetime chamber photon detectors.

The signal from the intermediate lifetime species is an exponential decay, $\exp(-t/\tau)$. It will now be shown that the signal in the lifetime chamber resulting from short lived molecular products formed directly in front of the lifetime phototubes is a constant, independent of the detection port. The signal observed in the lifetime chamber will then have the form

$$I = I_o \cdot \exp(-t/\tau) + C \qquad (5)$$

This equation forms the basis for analyzing our lifetime data.

First, the oxidant number density in the lifetime chamber is not position-dependent. Considerable differential pumping is used to minimize the oxidant number density in the lifetime chamber; the lifetime chamber is separated from the interaction region by two differentially pumped regions, the region closest to the lifetime chamber being pumped by an ion pump and operating at a pressure of less than $1 \cdot 10^{-7}$ torr. The lifetime chamber is pumped moderately poorly by a diffusion pump, but there is very little gas load due to the differential pumping. Furthermore, a liquid nitrogen cryopump is used in the lifetime chamber, and has been found to be very effective in removing N_2O oxidant. The baseline pressure in the lifetime chamber is approximately $3 \cdot 10^{-7}$ torr, and increases by approximately $1 \cdot 10^{-7}$ torr when the interaction region is filled with up to 10^{-3} torr of N_2O, the highest pressure used for lifetime measurements. At this pressure, no significant oxidant gradient can occur over the dimensions of the lifetime chamber. The source of oxidant in the lifetime chamber is the effusive flow from the interaction region. Such effusive flow does lead to a position dependent ($1/r^2$) oxidant number density in the lifetime chamber; given the dimensions of the apparatus, the interaction region pressure, and the differential pumping, however, it is easy to show that this contribution is much less than the background oxidant pressure. Hence the oxidant in the lifetime chamber is a uniform density corresponding to a partial pressure of about $1 \cdot 10^{-7}$ torr (approximately the vapor pressure of N_2O at liquid nitrogen temperature).

The metal atom beam which reaches the lifetime chamber is expanding so the flux (atoms/cm^2 sec) is decreasing as a function of distance. However, the viewing geometry of the phototubes on the lifetime chamber has been specifically designed so that all metal atoms which pass through the entrance aperture of the lifetime chamber remain within the viewing region of the detectors. (At these low lifetime chamber pressures, no substantial scattering occurs.) Hence the number of metal atoms passing through a plane in front of each detector in the lifetime chamber within the viewing range of the phototube is the same for each observation port.

In the lifetime chamber, then, there is an oxidant number density that does not change from port to port, and the total number of metal atoms passing in front of each tube within its viewing region is constant. Hence the time integrated number of photons from short lived species produced in front of each tube is constant. The solid angle subtended by a phototube is not significantly different from port to port. Hence, the same number of photons is detected at each port from this short lived source. *This is the key result.*

Given these considerations, the intensity observed at a port in the lifetime chamber should follow Equation (5). τ is the lifetime of the species formed in the interaction region and time decaying as it travels through the lifetime chamber, and C is a constant representing the contribution due to short lived species formed and emitting immediately in front of the lifetime chamber detectors. (A very long lived species would also contribute, weakly, to C.) Three parameters occur in Equation (5). Measurements are made at three different ports, so all three parameters can in principle be determined.

The reaction of samarium with N_2O offers an interesting test of this model. Sm + N_2O is a bright chemiluminescent reaction, but SmO chemiexcited states are short lived (τ = 83 ± 2 nsec)[7]. In our lifetime chamber, we observed three signals of equal intensity -- that is, no port-to-port variation. Furthermore, the ratio of the number of photons produced in the lifetime chamber to that produced in the interaction region was consistent with the ratio of the N_2O pressure in the lifetime chamber to that in the interaction region.

Two final procedural notes should be added. In performing the lifetime measurements, we have used three phototubes on the lifetime chamber, with a fourth tube on the interaction region used to normalize against shot-to-shot variations. In order to obtain reasonable statistics, we fire multiple shots for each measurement. In addition, to avoid comparing different tubes, we rotate all three tubes among all three ports, and therefore obtain three independent *sets* of data from which to calculate a lifetime.

Finally, it will be noted that there are three measurements used to obtain three parameters -- I_o, C and τ. Consequently, the fit is exact, and experimental error in the data is masked. This necessitates having good statistics in order to estimate uncertainties in the results. Because the signals in the lifetime chamber are weak, good statistics are difficult to obtain.

3.4.2 Screening Lifetime Technique

The difficulty of obtaining adequate data with good statistics to utilize the model presented in Section 3.4.1 is considerable. Within the context of the model, however, it is possible to make a set of screening measurements with much less difficulty; these screening studies can identify which molecules are worth further study.

Two procedures have been used, usually together. The first measurement examines the ratio of the signal observed in the interaction region (S_o) to that observed at the first lifetime port (S_1). If only short lived species produce light in the lifetime chamber, this ratio should equal the ratio of partial oxidant pressures in the two regions. If on the other hand, a long lived state is contributing significantly to the signal in the lifetime chamber, then S_o/S_1 should be *smaller* than the oxidant partial pressure ratio.

The second screening procedure compares the signal at the first port of the lifetime chamber (S_1) to the signal at the third port (S_3). According to the above development, a short lived state would give a ratio of one, but a contribution from a long lived state would make this ratio greater than one.

These techniques are much simpler to implement than the detailed lifetime analysis of Section 3.4.1 and are based on the same formalism. Such tests do not provide a lifetime, however; rather, they may be suggestive of the presence of a long lived chemiexcited state.

4.0 EXPERIMENTAL RESULTS

As is clear from the previous discussion, considerable effort has been expended in developing the experimental techniques and fully validating them. We feel confident this task is accomplished. Results presented in this section will demonstrate this to varying degrees. Because of the lack of time due to unexpected experimental delays, we have not obtained nearly as much data as we hoped. In particular, only N_2O was used as an oxidant in these studies. It should be recognized that changing the oxidant and performing the same sorts of experiments is fairly straightforward.

Experiments were carried out using N_2O and several metal atoms for each of the techniques discussed in Section 3. Because of the basic importance of information contained in the chemiluminescent spectra, these spectra were obtained for a considerable array of different metals (Section 4.3 and Table 3). The same array of metal atoms was subjected to screening lifetime experiments at the end of the contract, with some suggestive but incomplete results.

4.1 Chemiluminescent Reaction Stoichiometry

Determination of the chemiluminescent reaction stoichiometry is made as a part of the chemiluminescent cross section measurements. Results for several metals examined are summarized in Table 2. All chemiluminescent reactions we have examined are first order in both metal atom and oxidant under these conditions. The molecular products for the Nd and B chemiluminescent oxidation by N_2O are probably NdO and BO, respectively, but definitive spectroscopic assignments have not been made. Different reaction mechanisms may occur under different conditions; at higher oxidant pressures, for example, a reaction second order in oxidant could become dominant.

4.2 Cross Sections

4.2.1 Relative Chemiluminescent Cross Section

The relative chemiluminescent cross section for Ho, Pb, and Sn reacting with N_2O are shown in Figures 4, 5 and 6 respectively. For Ho, three different electronic states were identified in the chemiluminescent spectrum (see Section 4.3 and Table 5); Figure 4 shows the relative chemiluminescent

Table 2

Chemiluminescent Oxidation Reaction Stoichiometry

$$Ho + N_2O \rightarrow HoO^* + N_2$$

$$Sn + N_2O \rightarrow SnO^* + N_2$$

$$Pb + N_2O \rightarrow PbO^* + N_2$$

$$Sm + N_2O \rightarrow SmO^* + N_2$$

$$Fe + N_2O \rightarrow FeO^* + N_2$$

$$Al + N_2O \rightarrow AlO^* + N_2$$

$$Ge + N_2O \rightarrow GeO^* + N_2$$

$$Nd + N_2O \rightarrow \text{Products}^a + hr$$

$$B + N_2O \rightarrow \text{Products}^a + hr$$

[a] definitive spectroscopic assignment has not been made

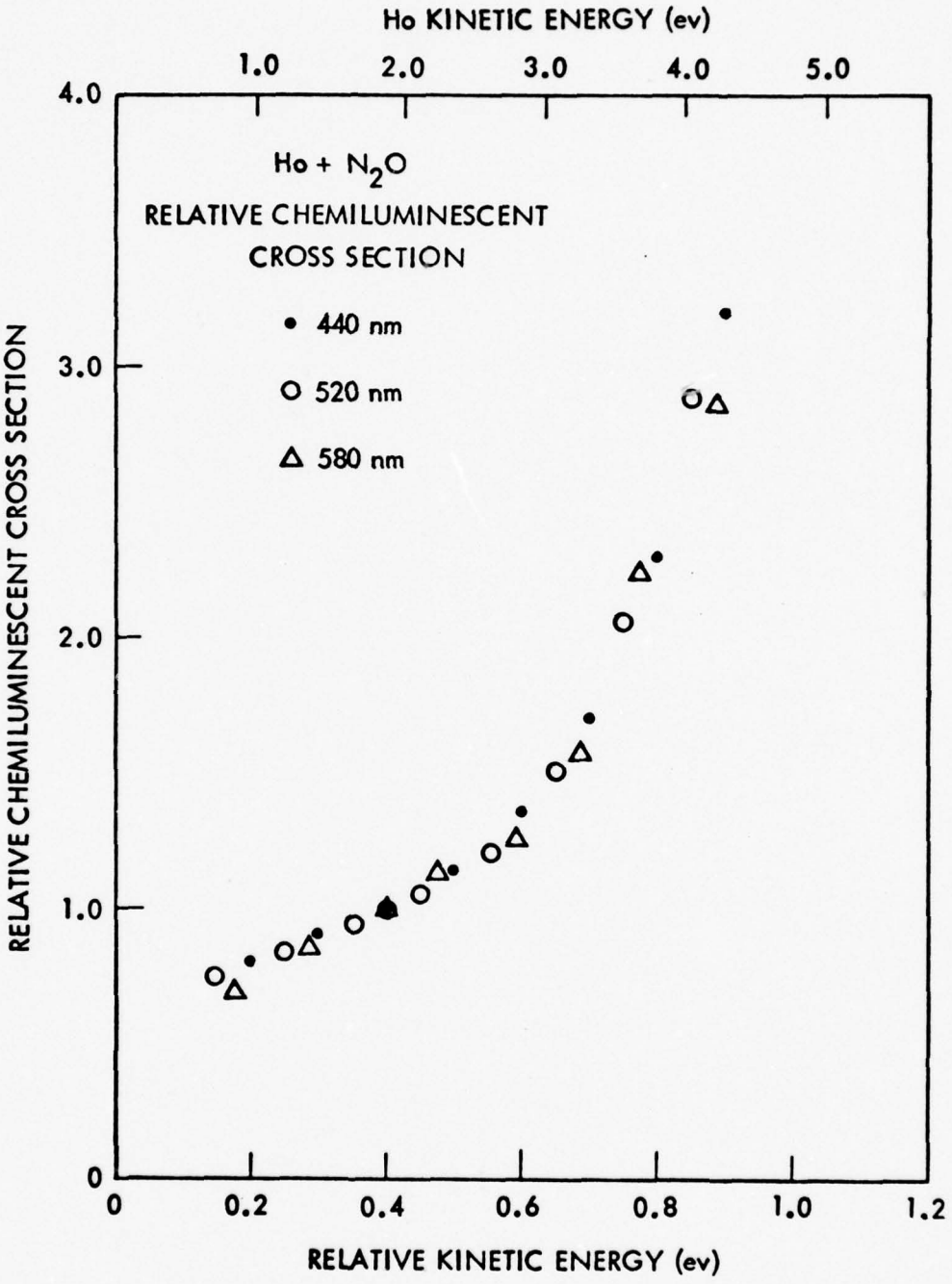

Figure 4. Relative chemiluminescent cross section vs. kinetic energy for the reaction Ho + N_2O → HoO* + N_2.

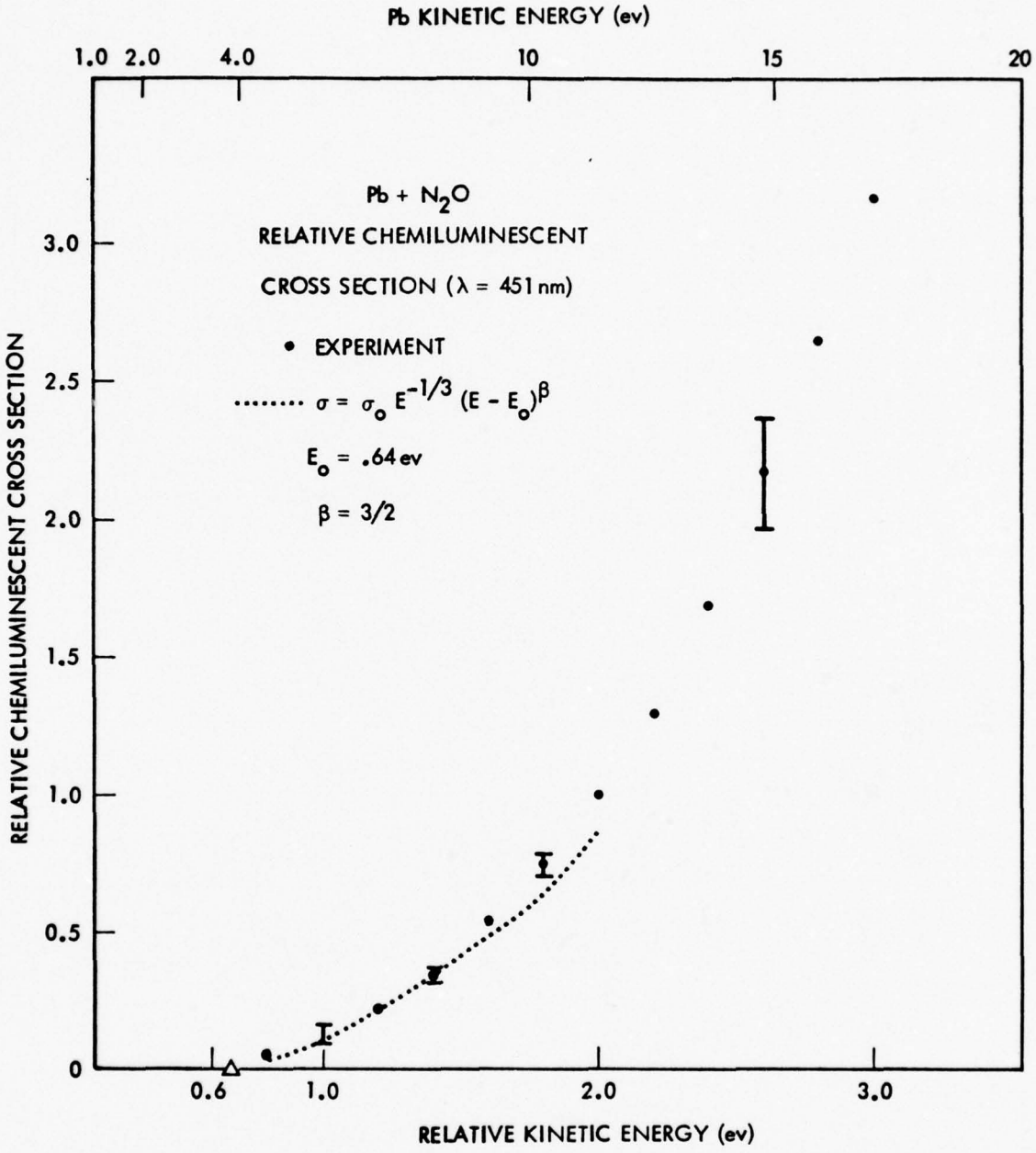

Figure 5. Relative chemiluminescent cross section vs. kinetic energy for the reaction Pb + N_2O → PbO(B,v'=0) + N_2.

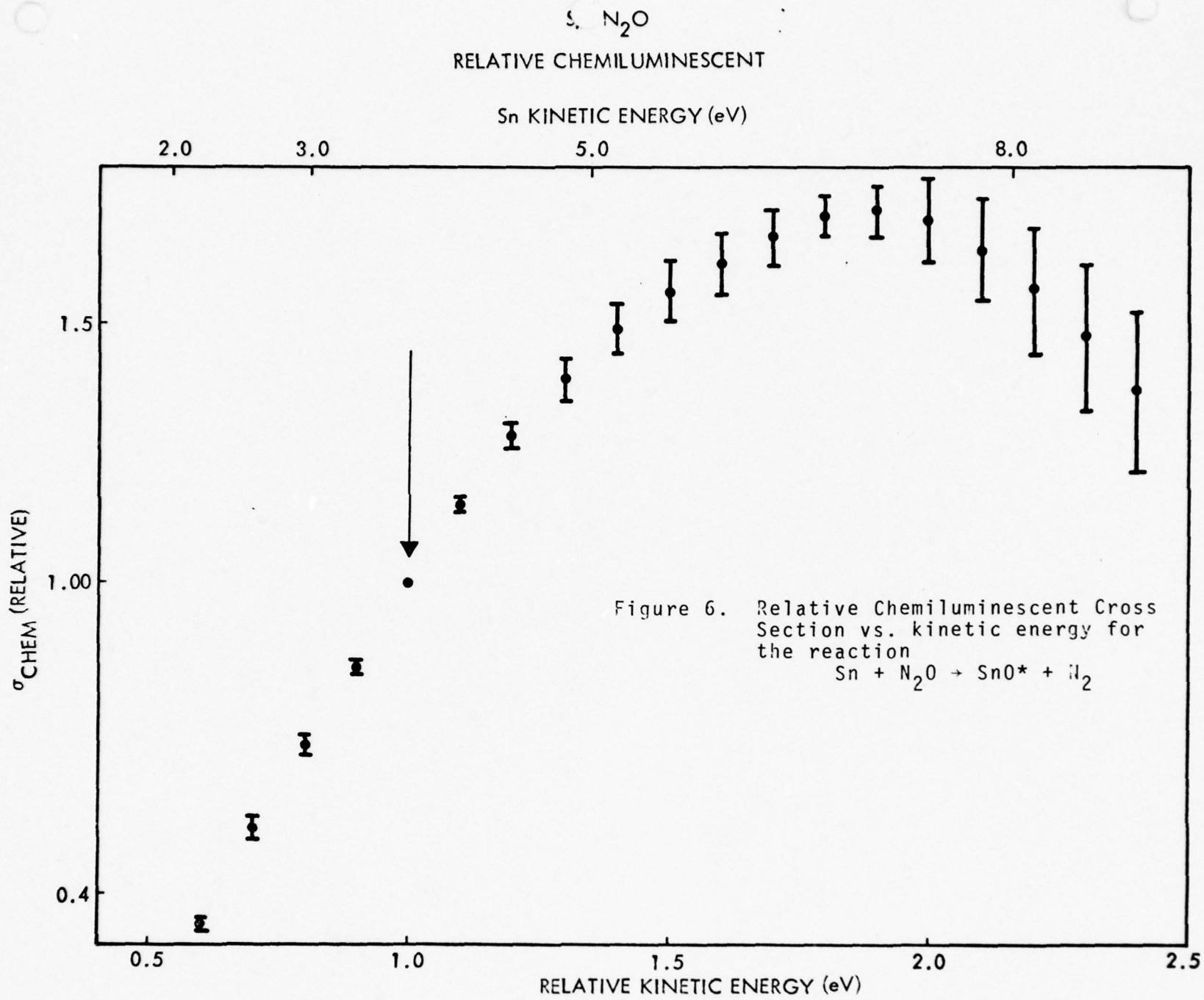

Figure 6. Relative Chemiluminescent Cross Section vs. kinetic energy for the reaction

$$Sn + N_2O \rightarrow SnO^* + N_2$$

cross section[8] for each of these states separately. (This result is described in more detail in Appendix B.) For the Pb oxidation reaction, wavelength specific photon detection was used to isolate the B-X (0-0) transition, so that the cross section[9] for forming PbO (B,v'=0) is obtained. The threshold corresponding to the reaction endothermicity is clearly evident. (This result is discussed in more detail in Appendix A.) The result for Sn was obtained using broad band photon detection.

4.2.2 Total Scattering Cross Section

The total scattering cross sections for Ho, Pb and Sn are shown in Figures 7, 8, and 9 respectively, as a function of kinetic energy. This total scattering cross section includes contributions from nonreactive scattering and reactions producing both chemiexcited and ground state molecules. Hence the total scattering cross section at a given kinetic energy represents an upper limit on the corresponding chemiluminescent cross section.

4.2.3 Total Reactive Cross Section

Data were obtained to calculate the total reactive cross section[8] for Ho + N_2O as outlined in Section 3.2.3. The reduced data and the least squares' fit to the data are presented in Figure 10. Note the linear increase in chemiluminescence at very low pressure, indicating the reaction is first order in oxidant. The computer fit to the data indicates a total reaction cross section of 16 ± 4 A^2. Note that this cross section includes contributions from reactive channels producing HoO* and HoO ground state. That this total reactive cross section is significantly smaller than the total scattering cross section (Figure 7) indicates that nonreactive scattering dominates this total scattering cross section.

4.3 Chemiluminescent Spectra

Considerable effort was made to obtain the chemiluminescent spectra for a large number of metal atoms reacting with N_2O. The success of this effort is the most significant accomplishment of the data collection aspect of this contract, and illustrates most convincingly the versatility of our experimental approach.

Table 3 summarizes the results of experiments using twenty different metal atom beams reacting with N_2O. Resolution of the spectra varied

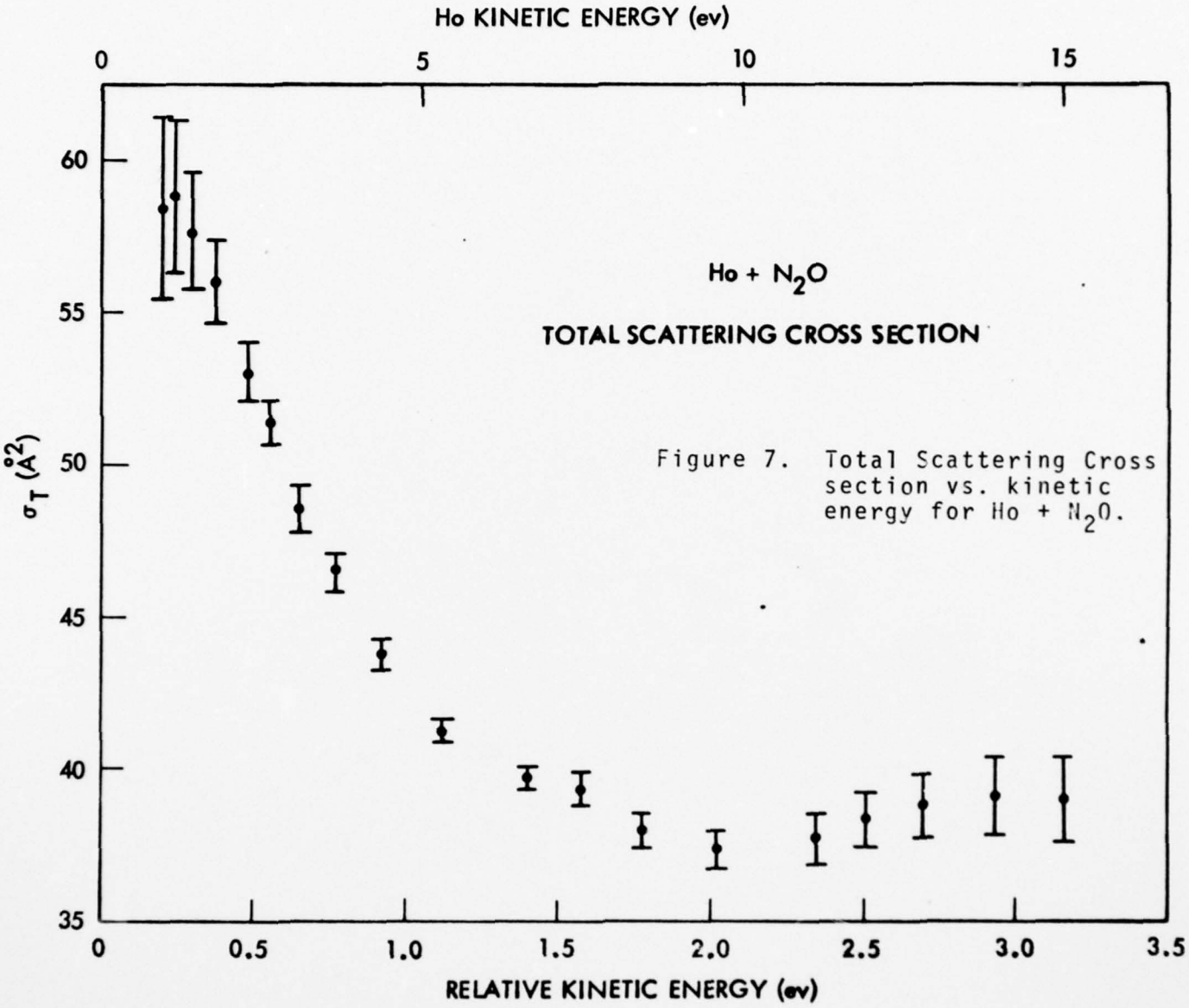

Figure 7. Total Scattering Cross section vs. kinetic energy for Ho + N_2O.

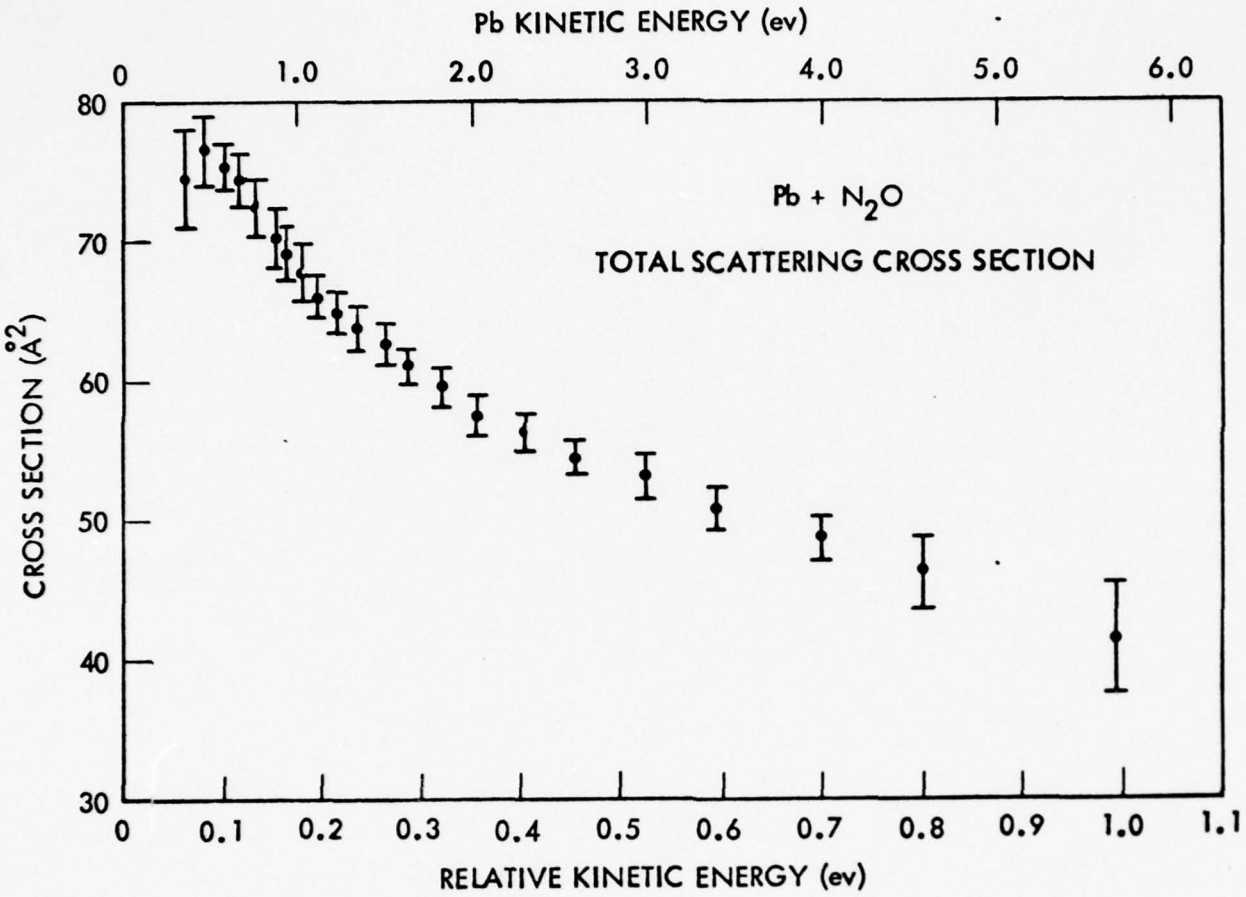

Figure 8. Total scattering cross section for Pb + N_2O.

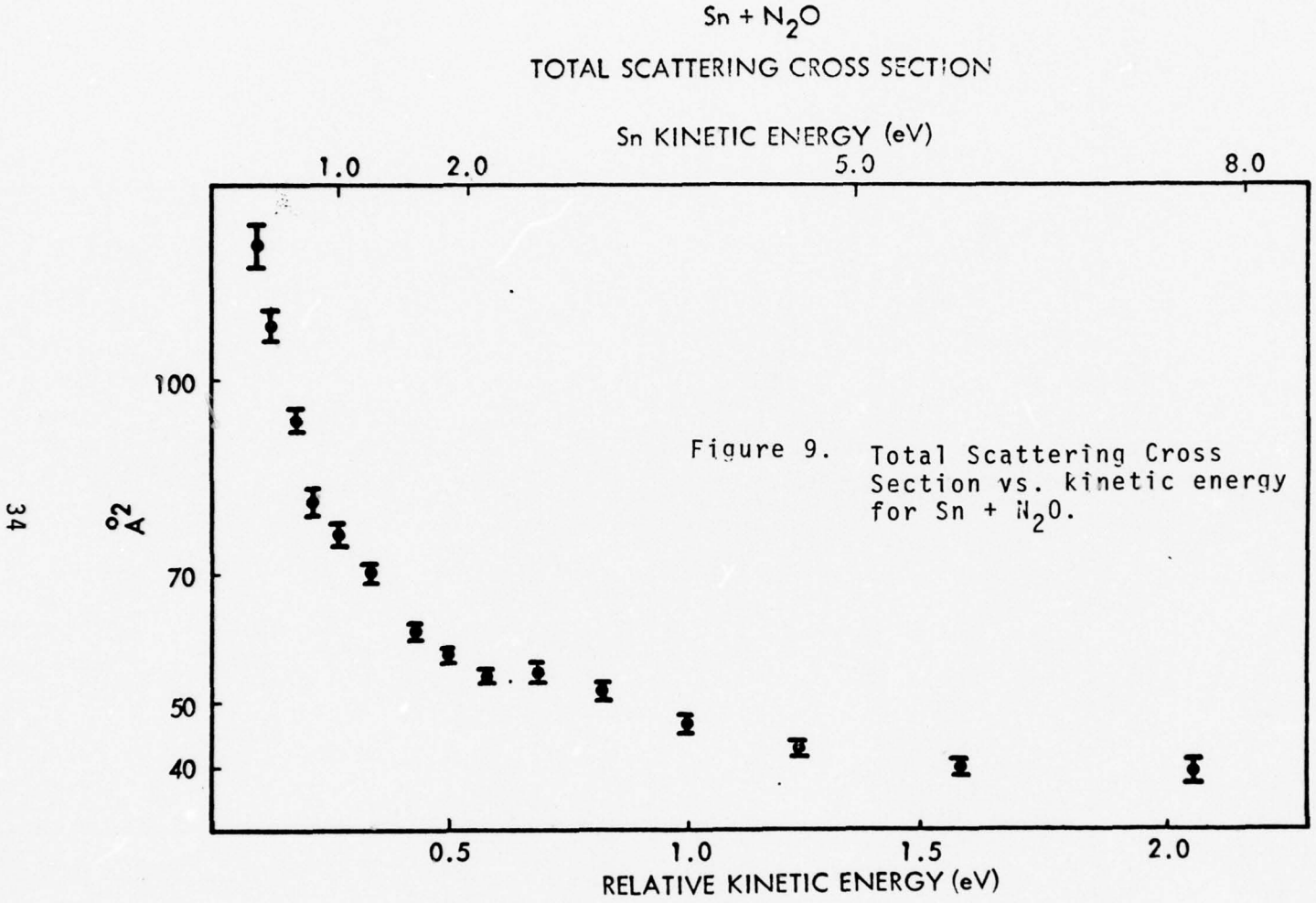

Figure 9. Total Scattering Cross Section vs. kinetic energy for Sn + N_2O.

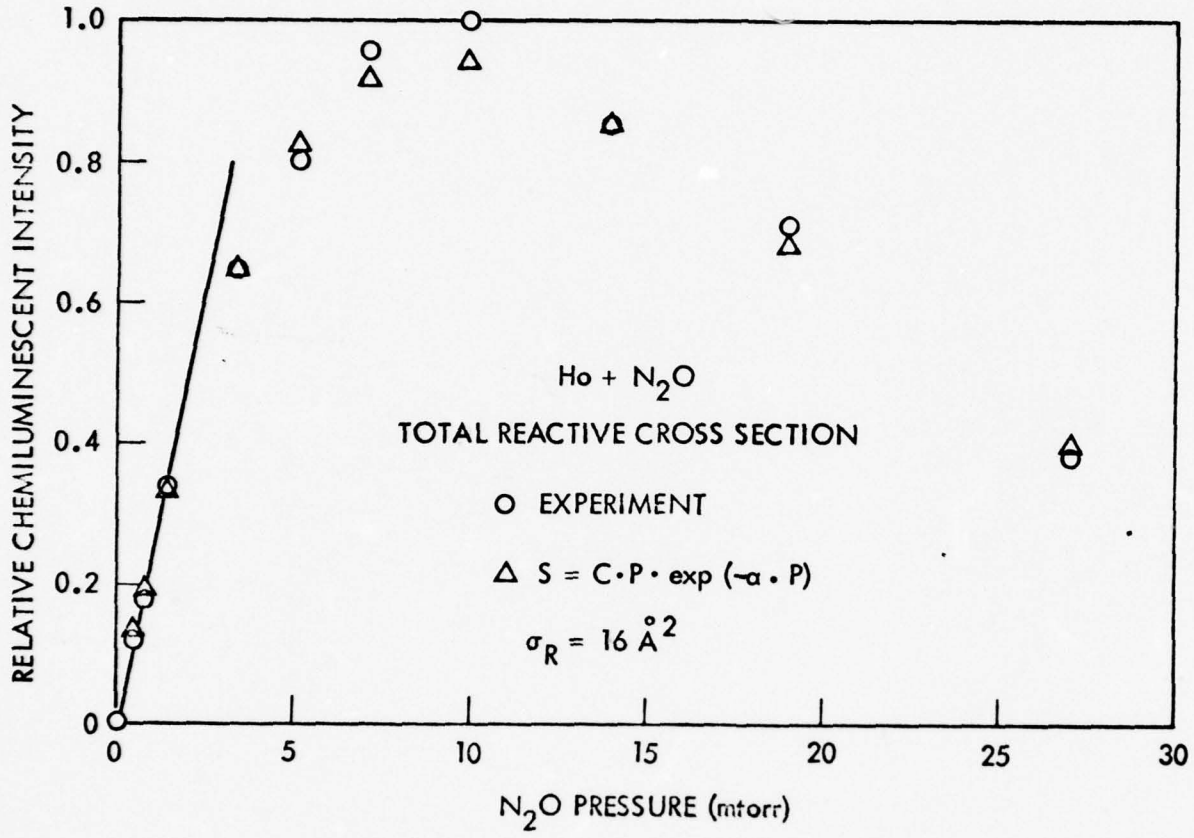

Figure 10. Total reactive cross section for Ho + N_2O.

Table 3

Metal Atom + N_2O Chemiluminescence Spectra

Summary of Results

Metal	Comments
Ho	3 distinct molecular transitions (one new electronic state)
La	C, B and D states of LaO
Ti	Broad emission from 400 nm to 700 nm
Fe	Broad emission with molecular structure (a and/or b states)
B	Broad emission with minor structure from below 400 nm to above 650 nm
Pb	Broad emission near 450 nm, structured toward red (B and a states)
Mg	Mg triplet emission, Na doublet emission; no molecular emission of any intensity
Sm	Broad emission centered near 470 nm, stronger emission with structure near 620 nm
Mo	Broad, structureless emission from 400 nm to 700 nm
Co	Atomic emission at 412 nm, broad emission from 400 nm to 640 nm with some structure
Ni	Broad emission from 420 nm to 640 nm
In	Strong atomic emission, weak molecular emission near 430 nm
Al	Strong stomic emission at 395 nm, structured emission from 420 nm to 560 nm (B)
Ge	Weak emission from 380 nm to 550 nm, considerable structure (B state)
Si	Very weak, broad emission, minor structure
Au	No observed emission
Nd	Broad, structureless emission from 400 nm to 570 nm
Mn	Broad, structured bands from 450 nm to 630 nm (A state)
Sn	Broad, structured emission from 360 nm to 525 nm (B, C states)
Cr	Broad emission from 420 nm to 680 nm, with considerable structure (B states)

from 0.1 nm in a few cases up to 4 nm. The information desired from the chemiluminescent spectra is identification of the electronic states populated by the reaction, not detailed analysis of the spectra. The state assignments have been obtained by comparison with standard spectroscopic reference works.[10] In several cases no state assignment is known.

These chemiluminescent spectra were obtained using an N_2O pressure of from 0.1 millitorr to 10 millitorr depending on the metal atom. Although some vibrational structure is seen on many of the spectra, most spectra contained broad emission.

The only totally uninteresting spectrum is that of Au + N_2O; absolutely no emission could be observed for this reaction, either using the OMA or using a broad band photomultiplier. We did not look for AuO product with the quadrupole mass spectrometer, unfortunately, so we are uncertain if any reaction takes place at all.

Ho + N_2O is one of the brightest chemiluminescent spectra we have examined. (Sm + N_2O is almost as intense.) The chemiluminescent spectrum[8] for Ho + N_2O is shown in Figure 11. Three broad electronic features are evident. The two transitions at longer wavelength have been observed previously,[11] but the short wavelength transition has not been previously reported[10] to our knowledge. All three features result from the bimolecular reaction of Ho with N_2O, and all show the same kinetic energy dependence in the chemiluminescent cross section (Figure 4). Chemiluminescent spectra of this new transition were obtained with 0.1 nm resolution, but even at this resolution little structure could be observed. Structure has been reported[11] for the higher wavelength transitions, although we see only faint indications of such vibrational features in our spectra at these low pressures.

The chemiluminescent spectrum for Sm + N_2O is shown in Figure 12. Resolution in this spectrum is approximately .5 nm. This spectrum is very similar to that reported recently by Dickson, et al.[12] They report a quantum yield for this reaction of 0.4%, a surprisingly low value considering that this is the second brightest chemiluminescent reaction we have observed in this work.

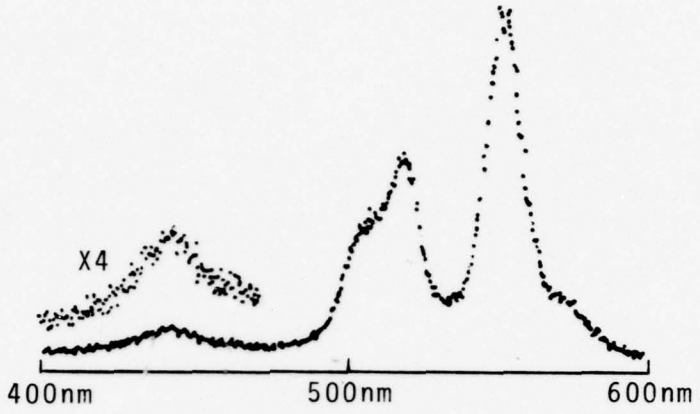

Figure 11. Chemiluminescent spectrum for $Ho + N_2O \rightarrow HoO^* + N_2$ (uncorrected for instrument response). Resolution ≈ 0.4 nm.

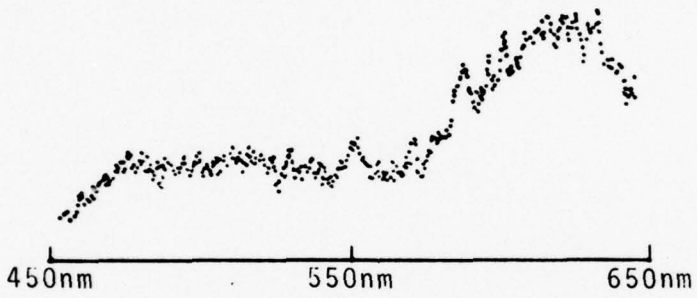

Figure 12. Chemiluminescent spectrum for $Sm + N_2O \rightarrow SmO^* + N_2$ (uncorrected for instrument response). Resolution ≈ 1. nm.

Figures 13 through 16 present the chemiluminescent spectra for N_2O oxidation of Mn, Al, Fe and Cr, respectively, Obvious identifiable structure is present in each spectrum.

Mg + N_2O is interesting in that no molecular emission could be detected, although the sodium doublet at 589 nm and a triplet-triplet transition in magnesium at 518 nm were observed; the sodium emission was about a factor of three more intense than the magnesium emission. Sodium probably originates from a contamination in the magnesium sample, although it could come from the glass substrate used in making the thin film targets. The magnesium transition originates from a ^3S state 41,197 cm^{-1} above the ground state.[13] In the absence of oxidant, no emission of any kind was observed. When the N_2O was replaced with argon, no emission occurred. Apparently the magnesium and sodium excited states are being populated by collision with a molecule with considerable internal energy which itself does not emit. Sodium is apparently populated in a spin conserving way. If magnesium is also populated by spin conservation, this would imply the lower level from which the ^3S is popululated is the metastable ^3P level.[13] Benard, et al[14] have reported that Mg (^3P) reacts very efficiently with N_2O to produce MgO molecular chemiluminescence, however, and we do not observe any MgO chemiluminescence. Appearance of the sodium and magnesium atomic emission lines under these conditions is most interesting and deserves further study.

In + N_2O is similar in that the most intense emissions observed are two In atomic transitions,[13] at 410 nm (^2S-$^2P_{1/2}$) and 451 nm (^2S-$^2P_{3/2}$). Much weaker InO emission (less than one tenth the atomic emission) is also observed near 430 nm (A-X). Again, removal of the oxidant eliminated the emission, and replacing the oxidant with an equivalent pressure of argon eliminated the emission. Occurence of this atomic emission may indicate the presence of an energy reservoir state which can efficiently excite atomic In in a collision but does not itself emit efficiently.

4.4 Lifetime Measurements

Early in the contract, the lifetime model was developed and thoroughly tested on the reaction Pb + $N_2O \rightarrow PbO^* + N_2$. Late in the contract the lifetime apparatus was reassembled, but mechanical difficulties and a lack

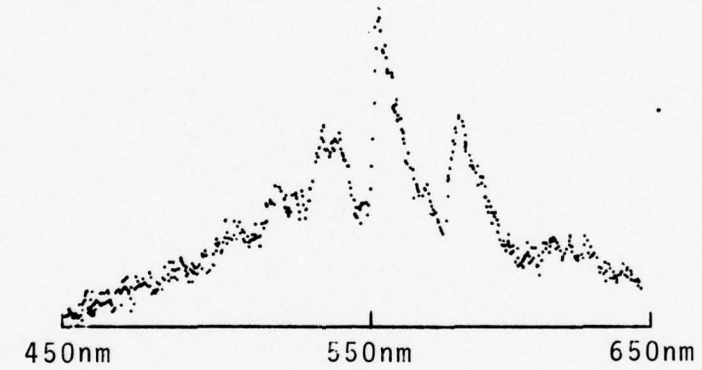

Figure 13. Chemiluminescent Spectrum for Mn + N_2O → MnO* + N_2 (uncorrected for instrument response). Resolution ≈ 1. nm.

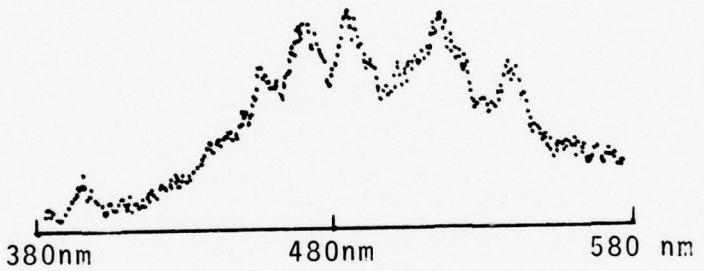

Figure 14. Chemiluminescent spectrum for $Al + N_2O \rightarrow AlO^* + N_2$ (uncorrected for instrument response). Resolution ≃ 4. nm.

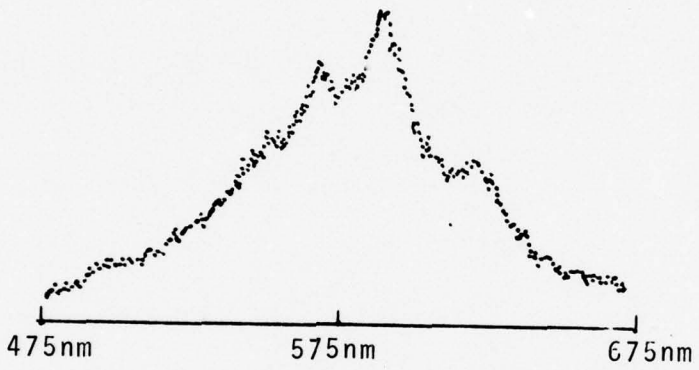

Figure 15. Chemiluminescent spectrum for $Fe + N_2O \rightarrow FeO^* + N_2$ (uncorrected for instrument response). Resolution ≃ 1. nm.

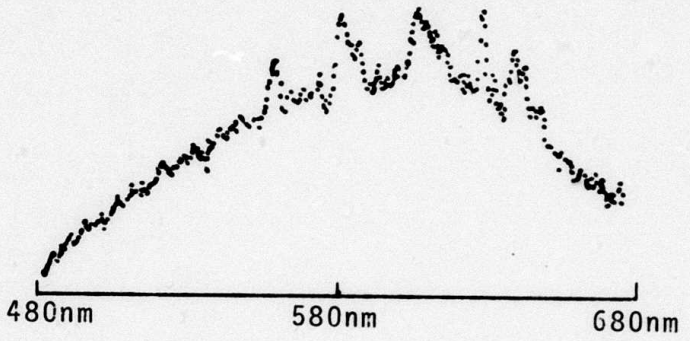

Figure 16. Chemiluminescent Spectrum for $Cr + N_2O \rightarrow CrO^* + N_2$ (uncorrected for instrument response). Resolution ≈ 1. nm.

of time have prevented our obtaining other statistically significant lifetimes. Instead, the two screening tests described in Section 3.4.2 have been used to obtain limited information on a number of metal atom reactions with N_2O. The difficulties associated with the lifetime experiments undertaken at the end of the contract appear to result from much weaker signals than were obtained previously, and correspondingly poor statistics.

The lead experiments represent the most complete measurement and analysis for a lifetime we have made. The ratio of the intensity in the interaction region (S_0) to that at the first port in the lifetime chamber (S_1) is 220, the lowest value we have observed for any metal. The ratio of the signal at the first port in the lifetime chamber (S_1) to the signal at the third port (S_3) is $S_1/S_3 \approx 2.5$. Both these screening tests indicate the presence of a long lived state decaying in the lifetime chamber.

Detailed lifetime data were collected for the Pb + N_2O reaction using the method outlined in Section 3.4.1. A data set for each of three phototubes was obtained; these data sets are presented in Table 4. Note that the signal for each tube in normalized to one at the first port. The statistics represent estimates based on at least five measurements in each position.

Table 4

PbO a Lifetime Data

Phototube	Relative Signal Port #1	Port #2	Port #3
4282-02	1.00	.63 ± .05	.44 ± .04
4282-03	1.00	.63 ± .05	.40 ± .04
4282-R	1.00	.60 ± .02	.43 ± .04
	1.00	.62 ± .02	.42 ± .02

PbO (a) lifetime $\tau = 49 \pm 10$ μsec

Analysis of these data according to the model of Section 3.4.1 gives a lifetime of 49 $\pm$ 10 μsec. The model further shows that 20% of the photons observed at the first lifetime port are due to a short lived contribution.

An interesting result was obtained by performing the same experiment but without liquid nitrogen cryopumping in the lifetime chamber. This experiment gave a slightly longer but statistically identical lifetime (62 $\pm$ 15 μsec), with a background contribution at the first lifetime chamber port of 50%. As expected, removal of the liquid nitrogen cryopump increased the background oxidant number density and therefore increased the photon contribution from the short lived state.

We assign the lifetime 49 $\pm$ 10 μsec to the a state of PbO; the background contribution appears to be PbO B, which dominates the chemiluminescent spectrum, although PbO A may also contribute to the background. Lifetimes of the A and B states of PbO have been measured[15] as 3.75 μsec and 2.58 μsec, respectively.

Dye laser induced fluorescence experiments and a Stern-Volmer analysis have recently been used by Brom, Revelli and Beattie[16] at the University of California at Santa Barbara to examine the PbO a lifetime. They find 82 $\pm$ 6 μsec for v'=3 and 61 $\pm$ 14 μsec for v'=4, the only vibrational levels they were able to monitor. Our broad band photon detection would include decay from all populated vibrational levels of PbO a. The large vibrational level dependence observed by Brom, et al[16] consequently compromises a direct comparison of our results, but the respective measurements do seem to be consistent. One additional state of PbO, the b state, is known to emit in the visible. Its lifetime is suspected to be considerably longer than the PbO a lifetime,[15] and has not been measured.[16] PbO b could contribute a small signal in our experiment, but this is thought to be unlikely.

Our recent experiments have concentrated on obtaining screening lifetime data for a variety of metal reactions with N_2O. The results of the screening experiments are summarized in Table 5. Species in the first column of this table had large values of S_0/S_1, and $S_1/S_3 \simeq 1$. Both measurements indicate no significant long lived contribution.

Species in the third column gave signals in the lifetime chamber too

weak to use even in the screening analysis. It is unclear why the signals are so weak, although we suspect somewhat deteriorated targets to be part of the problem.

The screening data for the center column molecules are given at the bottom of Table 5. The data for HoO are disconcerting; S_1/S_3 suggests a long lived contribution, and S_o/S_1 does not. It is not clear what interpretation to make of this! For the other three molecules, both screening measurements indicate the presence of a long lived emitter. It is interesting that PbO, SnO and GeO all involve metal atoms from the fourth column of the periodic table. (SiO is known to have a very long lived excited state.) Matrix isolation experiments[17] on SnO suggest a gas phase radiative lifetime of 330 μsec, significantly longer than we would expect on the basis of the preliminary data in Table 5. It is unfortunate that time has escaped us before these long lived species could be examined further.

Table 5

Lifetime Survey Results

only short lived species observed	long lived species present	too weak to study
SmO	HoO (?)	FeO
LaO	SnO	CrO
Co + N_2O	MoO	MnO
	GeO	AlO
		Ti + N_2O
		Si + N_2O
		B + N_2O
		Ni + N_2O

	S_1/S_3	S_o/S_1
HoO	1.8 ± .3	2500 ± 600
SnO	2.6 ± .4	875 ± 125
MoO	2.3 ± .3	375 ± 300
GeO	2.3 ± 1.	850 ± 250

5. SUMMARY

Laser vaporization of thin metal films has been used as the metal atom beam source for the study of chemiluminescent reactions. Experimental techniques have been developed and demonstrated to allow measurement of the chemiluminescent reaction stoichiometry, the relative chemiluminescent cross section vs kinetic energy, the total scattering cross section vs kinetic energy, the total reactive cross section (under favorable conditions), the chemiluminescent spectrum, and radiative lifetimes between approximately 10 and 100 μsec. The versatility of this laser vaporization metal beam source has been vividly demonstrated by obtaining the chemiluminescent spectra for the N_2O oxidation of twenty metal atoms under essentially identical experimental conditions. A definitive measurement of the PbO a lifetime has been made using our time-of-flight technique; we find PbO a lifetime $\tau = 49 \pm 10$ μsec. Lifetime screening experiments suggest that Sn, Mo and Ge reactions with N_2O appear to produce long lived chemiexcited states.

A major success of this program has been the development and testing of experimental techniques. Work on subsequent contracts would be devoted to using these techniques to acquire data. A significant array of data on metal atom chemiluminescent reactions would be obtained in the next months of experimentation.

6. REFERENCES

1. J.F. Friichtenicht, Review of Scientific Instruments 45, 51 (1974).

2. N.G. Utterback, S.P. Tang and J.F. Friichtenicht, Physics of Fluids, 19, 900 (1976).

3. S.P. Tang, N.G. Utterback and J.F. Friichtenicht, Journal of Chemical Physics, 64, 3833 (1976).

4. See, for example: M. Inghram and J. Drowart, High Temperature Technology, McGraw Hill, New York (1960); J. Drowart and P. Goldfinger Angew. Chem. 6, 581 (1967); J. Kordis and K.A. Gingerich, Journal of Chemical Physics 66, 483 (1977); E. Murad and D.L. Hildebrand, Journal of Chemical Physics 65, 3250 (1976).

5. C. Ottinger and R.N. Zare, Chemical Physics Letters 5, 243 (1970).

6. J.F. Friichtenicht and S.P. Tang, Paper 1.7, Proceedings of the Second Summer Colloquium on Electronic Transition Lasers, Woods Hole, Massachusetts, September 17-19, 1975.

7. C.R. Dickson, Ph.D. Thesis, Columbia University (1976).

8. S.P. Tang, B.G. Wicke and J.F. Friichtenicht, Journal of Chemical Physics, submitted for publication (see Appendix B).

9. B.G. Wicke, S.P. Tang and J.F. Friichtenicht, Chemical Physics Letters, accepted for publication (see Appendix A).

10. S.N. Suchard, Spectroscopic Constants for Selected Heteronuclear Diatomic Molecules, Aerospace Report No. TR-0074-(4641)-6 (1974); R.W.B. Pearse and A.G. Gaydon, The Identification of Molecular Spectra, Chapman and Hall, London (1976); G. Herzberg, Molecular Spectra and Molecular Structure, D. Van Nostrand, Princeton (1950).

11. A. Gatterer, Ricerche Spettroscop. Lab. Astrofis, Specola Vaticana 1, 139 (1942).

12. C.R. Dickson, S.M. George and R.N. Zare, Journal of Chemical Physics 67, 1024 (1977).

13. Wm. F. Meggers, Table of Spectral Line Intensities, N.B.S. MN 145, National Bureau of Standards (1975).

14. D.J. Benard and W.D. Slafer, Journal of Chemical Physics 66, 1017 (1977); D.J. Benard, W.D. Slafer and J. Hecht, Journal of Chemical Physics 66, 1012 (1977); D.J. Benard, W.D. Slafer and P.H. Lee, Chemical Physics Letters 43, 69 (1976).

15. R.C. Oldenborg, C.R. Dickson and R.N. Zare, Journal of Molecular Spectroscopy 58, 283 (1975).

16. J.M. Brom, M.A. Revelli, and W.H. Beattie, Journal of Molecular Spectroscopy, *submitted for publication (private communication)*.

17. B. Meyer, J.J. Smith and K. Spitzer, Journal of Chemical Physics 53, 3616 (1970).

Appendix A

Velocity Dependence of the $Pb + N_2O \rightarrow PbO(B,v=0) + N_2$ Chemiluminescent Reaction*

B.G. Wicke, S.P. Tang and J.F. Friichtenicht

TRW Systems Group
One Space Park
Redondo Beach,
California 90278

*Work supported in part by the Defense Advanced Research Projects Agency under U.S. Naval Research Laboratory Contract No. N00173-76-C-0258 and in part by TRW DSSG Independent Research and Development.

Abstract

We have used the technique of Q-switched ruby laser vaporization of thin metal films to obtain the velocity dependence of the reactive cross section for $Pb + N_2O \rightarrow PbO\ (B,v'=0) + N_2$ for kinetic energies in the vicinity of the thermodynamic threshold up to 3 eV (in the center of mass). The kinetic energy dependence is in good agreement with a statistical model. This experimental technique should be applicable to a wide variety of chemical kinetic studies.

I. Introduction

The dependence of chemical reactions on the kinetic energy of the reactants has been of considerable recent interest.[1] The development of the technique of seeded supersonic beam generation[2] has made it possible to study the effects of reactant kinetic energy up to several eV.[3] Simply stated, in a seeded beam source the reactant of interest is mixed with a very large excess of light atom (He) or molecule (H_2) and the mixture is expanded through a supersonic nozzle. As the fraction of the reactant decreases, the mass flow velocity of this reactant approaches the mass flow velocity of the diluent, with a corresponding kinetic energy increase approaching mass (reactant)/mass (diluent). The high intensity (10^{16} atoms/sr-sec) and the relatively narrow energy spread of the kinetic energy distributions ($\Delta E/E \approx 15\%$) are two significant features of the seeded supersonic beam source. Charge exchange[4] and sputtering[5] techniques have been used to a much smaller extent in studying kinetic energy dependent cross sections in this chemically interesting kinetic energy region.

We are developing a different technique for studying the kinetic energy dependence of various chemical kinetic phenomena involving metal atoms and ions. The technique is laser vaporization of thin metal films.[6,7,8] As described in more detail below, the metal atom vapor source is produced by nearly instantaneous (< 80 nsec) vaporization of thin metal films. The metal vapor pulse so formed expands and travels down the atomic beam apparatus to an interaction region. The most striking difference between this laser vaporization technique and seeded supersonic expansion is that

laser vaporization is a pulsed source. Because of the instantaneous formation of the vapor cloud, kinetic energy information is obtained from the time variation of the interaction being monitored. Data on a wide range of kinetic energies are obtained from each shot; in the Pb experiments described here, kinetic energies in the range 0.2-15 eV are observed. Moreover, a wide variety of metal atom reactions can be studied with virtually no change in the apparatus by simply changing the thin metal film target.

We report here the use of this laser vaporization technique to examine the kinetic energy dependence of the chemiluminescent reaction

$$Pb + N_2O \rightarrow PbO(B,v=0) + N_2 \qquad 1.$$

This particular reaction is interesting because it is endothermic by approximately 0.6 eV; consequently, addition of kinetic energy to the reactant Pb allows observation of the threshold dependence of the reactive cross section.

Section II describes the laser vaporization source in more detail as well as the atomic beam apparatus. The experimental results are presented and discussed in Section III.

II. Experimental

A. Laser Vaporization Source

Laser vaporization of thin metal films as a source of metal atoms has been described in detail previously.[6] Briefly, a target of the metal atom of interest is prepared by vapor deposition of a thin film (typically one micron) of the metal on a transparent substrate, usually an ordinary micro-

scope slide. Target preparation is a routine precedure; over two dozen different metal targets have been prepared and used. The target is suspended inside the source chamber of the atomic beam apparatus (see II.B) and irradiated through the transparent substrate by a Q-switched ruby laser pulse (λ = 6943 Å). Nominally 0.5 J incident energy is deposited on a 2 mm diameter spot in 80 nanoseconds; laser energy and focussed spot size are important variables in determining the kinetic energy of the resulting vapor cloud.[6,8] An extremely hot plasma is formed by this rapid deposition of energy on the opaque metal film. Because the plasma is confined initially between the substrate and the remaining metal film, very significant cooling takes place before the hot bubble "eats its way" through the film. (Much higher kinetic energies and substantial ionization result when the thin metal film target is irradiated from the front side instead of through the substrate.[8]) After vaporizing the entire thickness of the film, the expanding cloud of metal vapor becomes collisionless within several cm of the target. The atomic beam pulse is then collimated and swept free of ions if necessary. (No detectable ions were observed in the Pb studies reported here, although Pb^+ can be made by front surface laser vaporization.[8])

Depending on the material, the film thickness, and the focussed spot size, a pulse of nominally 10^{17} atoms is formed.[6] Because the center of mass of the expanding vapor cloud is itself moving away from the substrate with substantial velocity,[8] atomic fluxes downstream can be much larger than simple solid angle ratios would predict. Time integrated fluxes $\geq 10^{15}$ atoms/cm^2 can be obtained 10 cm away from the target.

B. Atomic Beam Apparatus

The essential features of the atomic beam apparatus have been described previously.[7] The metal source is simply the thin-film coated microscope slide suspended in the source chamber. As currently used, the interaction region is a small chamber filled with a low pressure (typically 0.5 m torr) of oxidant. The interaction region has small entrance and exit channels for the atomic beam and molecular products, and several quartz windows for viewing chemiluminescence. A capacitance manometer is used to measure oxidant pressure in the interaction region. A pulsed nozzle source for the oxidant has been constructed and used as reported previously,[7] but was not employed in this study. All experiments described here were performed under single collision conditions as verified by monitoring attenuation of the metal atom beam using a quadrupole mass spectrometer located downstream from the interaction region.

Light emitted by chemiluminescent reactions in the interaction region can be monitored through the quartz windows. In this work, a bare phototube (with low gain) was used to monitor total chemiluminescence and a monochromator-phototube combination was used to monitor production of PbO (B,v=0) at 451 nm ($B(v'=0) \rightarrow X(v''=0)$).

Metal oxide product could also be detected using the quadrupole mass spectrometer. This was not done in the present experiments because the state-specific reaction cross section was desired.

III. Results and Discussion

The reaction of Pb + N_2O (with each reactant in its ground state) is sufficiently exothermic to produce PbO in the X, a and b states only.[9-12] Addition of energy to the reaction as Pb atom kinetic energy makes production of the A and B states energetically possible. As a routine part of our studies, the chemiluminescent spectrum of the Pb + N_2O reaction was obtained using this laser vaporization source and an optical multichannel analyzer. The chemiluminescent spectrum, taken with 2.0 nm resolution, shows broad, featureless emission between 400 nm and 500 nm (the region of the B-X transition) similar to that reported by Oldenborg et al.[9] for the Pb + O_3 reaction, and weak structured emission further to the red. One reason for the weakness of the red emission is the longer radiative lifetimes of the a and b states which emit in this region. Spontaneous emission lifetimes for PbO A and B states have been measured[9] by pulsed laser-induced fluorescence techniques as 3.8 usec and 2.6 usec, respectively. Lifetimes of a and b were too long to measure in those experiments;[9] the a state lifetime was estimated to be $\geq$ 10 usec. We have measured the a state lifetime of 49 $\pm$ 10 usec using a new time-of-flight technique to be reported elsewhere.[13] For a state with a short radiative lifetime, the observed chemiluminescence is simply proportional to the rate of formation of metal oxide molecules in the excited state. For a state with a long radiative lifetime, the photon flux is reduced. Furthermore, the reduction is exacerbated if the product molecule is moving rapidly. For PbO a with a radiative lifetime of 49 usec at a velocity of 5 eV (in the laboratory),

this reduction is approximately an order of magnitude. The b state, with its longer radiative lifetime (due to the b-X forbidden character in Hund's case c [9,14]) would be still weaker. The a-X and b-X features dominate the chemiluminescent spectra for the Pb + O_3 reaction reported by Olderborg et al.[9] because the B state is not energetically accessible for ground state reactants under those conditions.

The chemiluminescent reaction (1) is monitored by observing the chemiluminescence at 451 nm (2 nm FWHM slitwidth). This wavelength corresponds to the (0,0) bandhead of the B-X transition. It should be emphasized that the product state identification as B(v'=0) is based solely on this wavelength choice. Other higher lying levels may contribute to the monitored intensity at 451 nm, but especially at lower kinetic energies the dominant contribution to the 451 nm chemiluminescence should be from B(v'=0). This chemiluminescence is first order in the Pb flux as monitored independently by the quadrupole mass spectrometer. The chemiluminescence is also first order in the N_2O number density as monitored by the capacitance manometer at the low pressure limit of the chemiluminescence intensity.

The relative chemiluminescent cross section vs. kinetic energy for reaction (1) is measured by simultaneously monitoring the chemiluminescent emission at 451 nm vs. time and the metal atom flux vs. time. The chemiluminescence signal at time t is proportional to the flux of PbO(B,v=0) formed in the interaction region. The quadrupole mass spectrometer signal is proportional to the number density of Pb atoms at the ionizer. Straight forward corrections are made to change the number density observed at the ionizer to the incident metal atom flux in the interaction region. (Time corrections are included to account for the times spent by the metal ions

in the quadrupole.) The oxidant pressure in the interaction region was adjusted to insure that at each velocity the metal atom beam was attenuated by $\lesssim 5\%$ so that the observed metal signal accurately reflected the incident metal flux. The relative chemiluminescent cross section vs. kinetic energy is then obtained by dividing the chemiluminescent signal at the appropriate time by the properly corrected quadrupole mass spectrometer signal at the corresponding time. Numerous shots were taken to improve statistics.

The resulting cross section data are presented vs. kinetic energy in figure 1; the cross sections are arbitrarily normalized at 2.0 eV kinetic energy in the center of mass. Only relative cross sections have been obtained here because only the relative metal atom flux is known. Although the chemiluminescent cross sections are relative, the absolute values must be small; over the same range of kinetic energy where the chemiluminescent cross section increases by more than two orders of magnitude, the differential scattering cross section decreases from 50 to 40 A^2.

The chemiluminescent cross section data show a definite threshold at .62 $\pm$ .05 eV (in the center of mass). It is difficult to specify the threshold too accurately because of the vanishing intensity at threshold and the confusion with dark current. Increasing the phototube gain by $\approx$10 gave the same low energy dependence to the cross section.

Also plotted in figure 1 is a fit (for energy less than 2 eV) to the statistical model of Krenos and Tully.[14] The fit for energies below 1.5 eV kinetic energy is within experimental error. The fit at higher kinetic energy deviates significantly, at least in part because additional reactive channels may be available which can produce photons at 451 nm. The threshold of

0.62 ± .05 eV. Ignoring the small thermal energy of the room temperature oxidant, this observed threshold suggests a PbO bond dissociation energy of 3.8 ± .1 eV, in excellent agreement with the mass spectrometric result of 3.83 ± .05 eV.[11]

Oldenborg et al.[9] and Kurylo et al.[10] observed that metastable Pb ($^3P_1$ and $^3P_2$) reacted preferentially with O_3 to give PbO (B). If the experiments of Oldenborg et al.[9] were performed under truly single collision conditions, most of the observed PbO (B) emission ($\lambda < 440$ mm) is beyond the exoergicity limit of their reaction conditions; hence, except for the extreme high energy tail of their kinetic energy distribution, this PbO (B) emission must result from metastable Pb reactions. Oldenborg suggested that metastable Pb was formed by a small electrical discharge associated with their source heater assembly.[9,15] Kurylo suggested[10] that metastable lead was formed thermally in their source. Pb $^3P_1$ lies 7819 cm^{-1} = .97 eV above ground state $^3P_0$ lead. In our Pb + N_2O experiments, we observe essentially no B-X emission below 0.6 eV kinetic energy (figure 1) suggesting either that there is very little metastable Pb ($^3P_1$) present or that the reactive cross section

$$Pb(^3P_1) + N_2O \rightarrow PbO(B) + N_2 \qquad 2.$$

is extremely small in the kinetic energy region below 0.6 eV. We tend to favor this latter interpretaion, for the following reason. The source temperature in these laser vaporization experiments is not known and may not even be well defined.[8] Nevertheless, a Boltzmann equilibrium temperature of 2000°K would mean the $Pb(^3P_1)/Pb(^3P_0)$ ratio is 1%. Yet our experimental

sensitivity is such that the PbO(B) chemiluminescence at 0.5 eV is significantly less than 1% of that at 1.5 eV. Furthermore, the source temperature describing the kinetic energy distribution is significantly greater than 2000°K. Hence it seems unlikely that Pb ($^3P_1$)/Pb ($^3P_0$) is $<< 1\%$. The alternative explanation is that the cross section for reaction (2) is significantly smaller (for less than 0.6 eV kinetic energy) than the corresponding cross section for Pb($^3P_0$) at 1.5 eV kinetic energy. The reason for this suggested reaction specificity, like that in the Pb* + O_3 reaction,[9] is not understood.

These experiments with Pb indicate the usefulness of laser vaporization in studying the kinetic energy dependence of reactive cross sections. When chemiluminescence can be used as the molecular detector, the pulsed nature of the laser vaporization source is not a serious problem. Use of this metal atom source to study vibrational level-specific reactive cross sections in the ground state (when laser induced fluorescence is used for vibrational level specific detection) may be more problematical due to the low duty cycle of the ruby laser. An additional useful feature of this laser vaporization source is the ease with which many different metals as well as different oxidants may be studied under essentially identical conditions. Finally, more highly excited chemiluminescent states may be observed than in experiments using more conventional metal atom sources due to the considerable additional kinetic energy which can be added to the reaction exothermicity. These additional spectral features should be considered as "richness" rather than "complexity" because the velocity can be modified with relative ease.

References

1. See, for example: M.E. Gersh and R.B. Bernstein, J. Chem. Phys. 56, 6131 (1972); A.M.G. Ding, L.J. Kirsch, D.S. Perry, J.C. Polanyi and J.L. Schreiber, Faraday Discuss. Chem. Soc. 55, 252 (1973); D.L. King, D.A. Dixon and D.R. Herschbach, Faraday Discuss. Chem. Soc. 55, 331, 375 (1973); J.Am.Chem.Soc. 96, 3328 (1974); J.G. Pruett, F.R. Grabiner, and P.R. Brooks, J. Chem. Phys. 63, 1173 (1975); J.C. Polanyi, J.J. Sloan and J. Wanner, Chem. Phys. 13, 1 (1976); B.E. Wilcomb, T.M. Mayer, R.B. Bernstein and R.W. Bickes, Jr., J.Am.Chem.Soc. 98, 4676 (1976).

2. E.W. Becker and W. Henkes, Z.Phys. 146, 320 (1956); N.Abauf, J.B. Anderson, R.P. Andres, J.B. Fenn and D.G.H. Marsden, Science 155, 997 (1967).

3. R.A. Larsen, S.K. Neoh and D.R. Herschbach, Rev.Sci.Instrum. 45, 1511 (1974).

4. R.K.B. Helbing and E.W. Rothe, Rev.Sci.Instrum. 8, 1948 (1968)

5. J. Poletiek, P.K.Rol, J. Los and P.G. Ikelaar, Rev. Sci. Instrum. 8, 1147 (1968).

6. J.F. Friichtenicht, Rev.Sci.Instrum. 45, 51 (1974).

7. S.P.Tang, N.G. Utterback and J.F. Friichtenicht, J. Chem. Phys. 64, 3833 (1976).

8. N.G. Utterback, S.P. Tang and J.F. Friichtenicht, Phys. of Fluids 19, 900 (1976).

9. R.C. Oldenborg, C.R. Dickson and R.N. Zare, J. Mol. Spectros. 58 283 (1975).

10. M.J. Kurylo, W. Braun, S. Abramowitz and M. Krauss, Journal of Research of the National Bureau of Standards 80A, 167 (1976).

11. J. Drowart, R. Colin and G. Exsteen, Trans. Fara.Soc. 61, 1293 (1965).

12. C. Linton and H.P. Broida, J. Mol. Spectros. 62, 396 (1976).

13. B.G. Wicke, S.P. Tang and J.F. Friichtenicht, to be published. Work done at the Quantum Institute, University of California at Santa Barbara, gives $\tau(v'=3)=82$ usec and $\tau(v'=4)=61$ usec (J. Brom, Jr., M.A. Revelli and W. Beattie, private communication).

14. J.R. Krenos and J.C. Tully, J.Chem.Phys. 62, 420 (1975); see also L.W. Hall, J.Chem.Phys. 66, 2435 (1977).

15. B.G.Wicke, M.A. Revelli and D.O.Harris, J.Chem.Phys. 63, 3120 (1975).

16. It is possible that conditions near the metal atom target are such that no metastables survive the expansion. We are examining the population of metastable atoms produced by laser vaporization.

Figure Caption

Figure 1. $Pb + N_2O \rightarrow PbO^* + N_2$ relative chemiluminescent cross section (λ = 451 nm) vs kinetic energy. ⋮ experimental values, normalized at 2.0 ev (with representative error bars); •••• fit (at less than 2.0 ev) to a statistical model (reference 14).

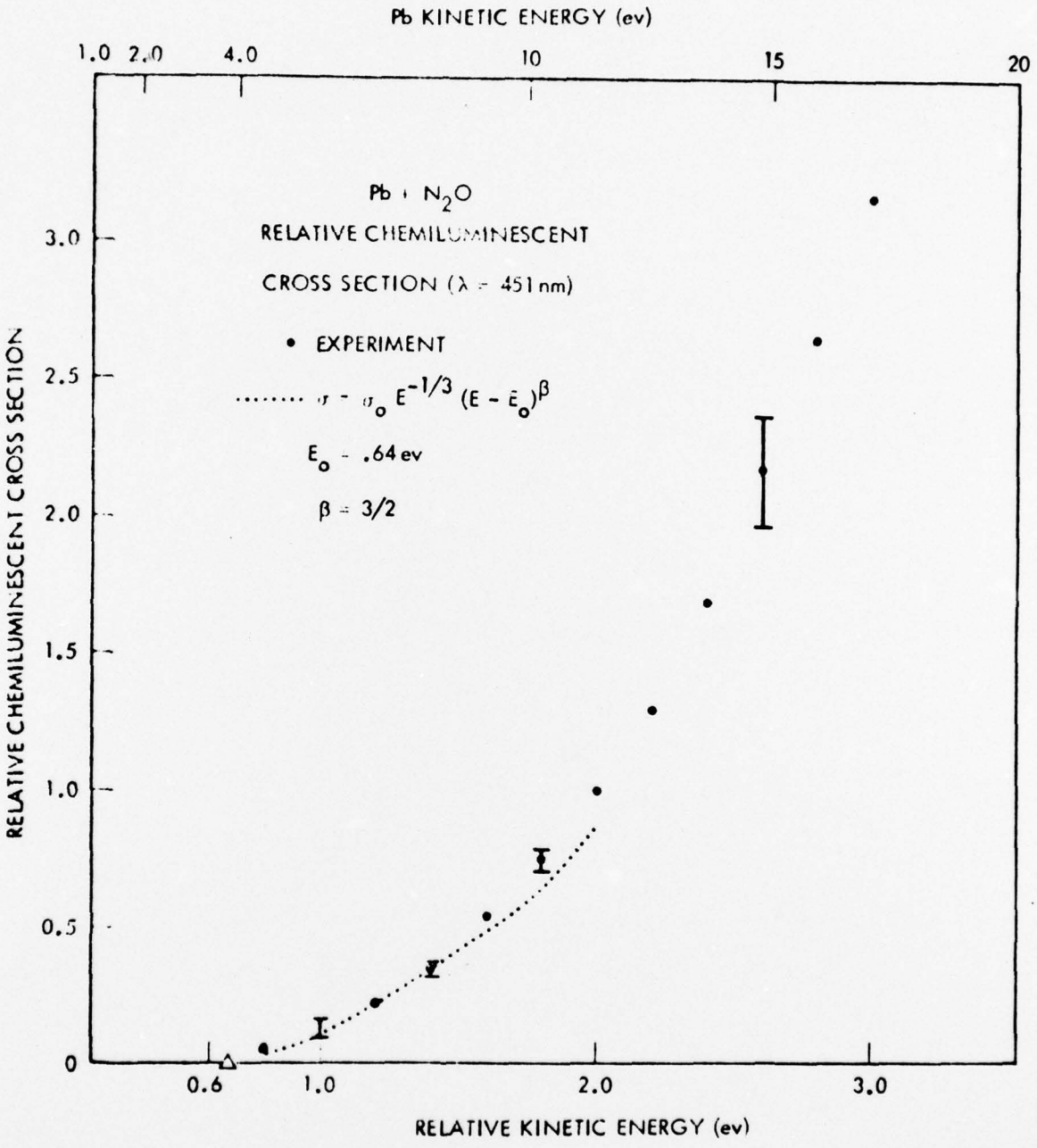
Pb KINETIC ENERGY (ev)
1.0
2.0
4.0
10
15
20
Pb + N_2O
RELATIVE CHEMILUMINESCENT
CROSS SECTION (λ = 451 nm)
• EXPERIMENT
..... $\sigma = \sigma_o E^{-1/3} (E - E_o)^{\beta}$
E_o = .64 ev
β = 3/2
RELATIVE CHEMILUMINESCENT CROSS SECTION
3.0
2.5
2.0
1.5
1.0
0.5
0
0.6
1.0
2.0
3.0
RELATIVE KINETIC ENERGY (ev)

Appendix B

STUDIES OF THE CHEMILUMINESCENCE REACTION

$$Ho + N_2O \rightarrow HoO^* + N_2$$

to be submitted as a note to
JOURNAL OF CHEMICAL PHYSICS

30 August 1977

S. P. Tang, B. G. Wicke and J. F. Friichtenicht

TRW
Defense and Space Systems Group
One Space Park
Redondo Beach, California 90278

Work supported in part by the Defense Advanced Research Projects Agency under U.S. Naval Research Laboratory Contract No. N00173-76-C-0258 and in part by TRW DSSG Independent Research and Development

A previous paper[1] reported measurement of the energy-dependent relative chemiluminescent cross section for the $Ho + N_2O \rightarrow HoO^* + N_2$ reaction where it was *assumed* that the observed optical emission derived from electronically excited HoO* molecules. This note presents spectroscopic verification of this assumption and gives the results of similar measurements for each of the three excited electronic states of HoO populated in the reaction. The velocity-dependent total scattering cross section σ_T, previously reported[1] on a realtive basis, has been reduced to an absolute measurement and the total reactive cross section σ_R has been measured as well.

The main features of the experimental apparatus and data acquisition and analysis procedures were described in Reference 1. Briefly, the Ho atom beam was produced by the Q-switched ruby laser irradiation of a nominally 1 micron thick Ho film deposited on a transparent substrate. This technique[2] produces a pulsed beam such that the transit time of an atom from the substrate to a remote location specifies its velocity.

The collimated metal atom beam enters and exits the reactive region through small cylindrical channels. These channels also isolate the pressurized region ($P \leq .5$ mtorr) from the surrounding vacuum ($P \approx 10^{-7}$ torr). The transmitted atomic beam was monitored by means of a quadrupole mass spectrometer. In practice, the pressure in the reaction chamber is adjusted such that the Ho atom beam is attenuated by $\leq 5\%$, thereby ensuring single collision conditions. Chemiluminescence in the reaction zone was detected and analyzed with either a photomultiplier tube (PMT) or an optical multichannel analyzer (OMA).

The chemiluminescence spectrum of HoO obtained using the OMA with 0.4 nm resolution is shown in Figure 1. The spectrum shows three well resolved electronic transitions. The two longer wavelength transitions ($490 < \lambda < 550$ nm and $550 < \lambda < 600$ nm) have been observed previously[3] in a carbon arc, whereas the transition in the 400 to 490 nm region has not been reported previously. Spectra have been obtained at 0.1 nm resolution and we are currently attempting to perform a vibrational analysis of these data.

The relative chemiluminescent cross section for each electronic state has been determined by simultaneously measuring the wavelength-specific chemiluminescent emission and the metal atom flux as a function of transit time (i.e., metal atom velocity). A monochromator with 6.5 nm bandpass was used to record the chemiluminescent signals with the center wavelengths of 440, 520, and 580 nm chosen for the respective electronic transitions. Only relative chemiluminescent cross sections have been obtained because only the relative metal atom flux is available.

Data were analyzed as described in Reference 1. The energy dependences of the three state-specific chemiluminescent cross sections are shown in Figure 2. As is evident from this figure, there is no significant difference in the energy dependence of the cross sections among the three electronic states. It should be emphasized that each state is populated by a bimolecular reaction with no significant collisional quenching due to the low pressure in the reaction region.

The total scattering cross section was obtained by measuring the attenuation of the metal atom beam as a function of pressure in the interaction region (as monitored by a capacitance manometer). Knowledge of the oxidant number density and the effective scattering path length provides an

absolute total scattering cross section. Only relative values of σ_T were given in Reference 1 because of uncertainties in the effective target gas pressure. The current results agree with the previous results[1] and the value of σ_T at 0.63 ev center of mass energy (3 ev Ho kinetic energy) is $50 \pm 10\ A^2$.

Because the various cross sections are only weakly dependent on kinetic energy, it is possible to model the pressure dependence of the total light output of this chemiluminescent reaction. Total intensity vs. pressure increases at low pressure in a manner characteristic of the reaction stoichiometry, but decreases at higher pressure due to various beam attenuation processes.[4] For collisions involving a fast, heavy metal atom with N_2O, with a wide angle viewing geometry, and for processes with little or no kinetic energy dependence, the phenomenological attenuation cross section obtained in this modeling is the total reactive cross section. The result obtained in this way for Ho + N_2O is $16 \pm 4\ A^2$, representing both light producing and "dark" reaction products. Hence the total scattering cross section of $\simeq 50\ A^2$ is dominated by nonreactive scattering. The branching ratio for the three excited states of HoO is 1:.6:.1 in order of increasing excitation energy. We are not able to estimate the contribution of the reaction path producing ground state products.

Figure Captions

Fig. 1. HoO chemiluminescence spectrum measured with an optical multichannel analyzer. The bottom picture is an expansion of the top one showing clearly the transition of $400 < \lambda < 490$ nm.

Fig. 2. $Ho + N_2O \rightarrow HoO^* + N_2$ relative chemiluminescent cross sections vs kinetic energy.

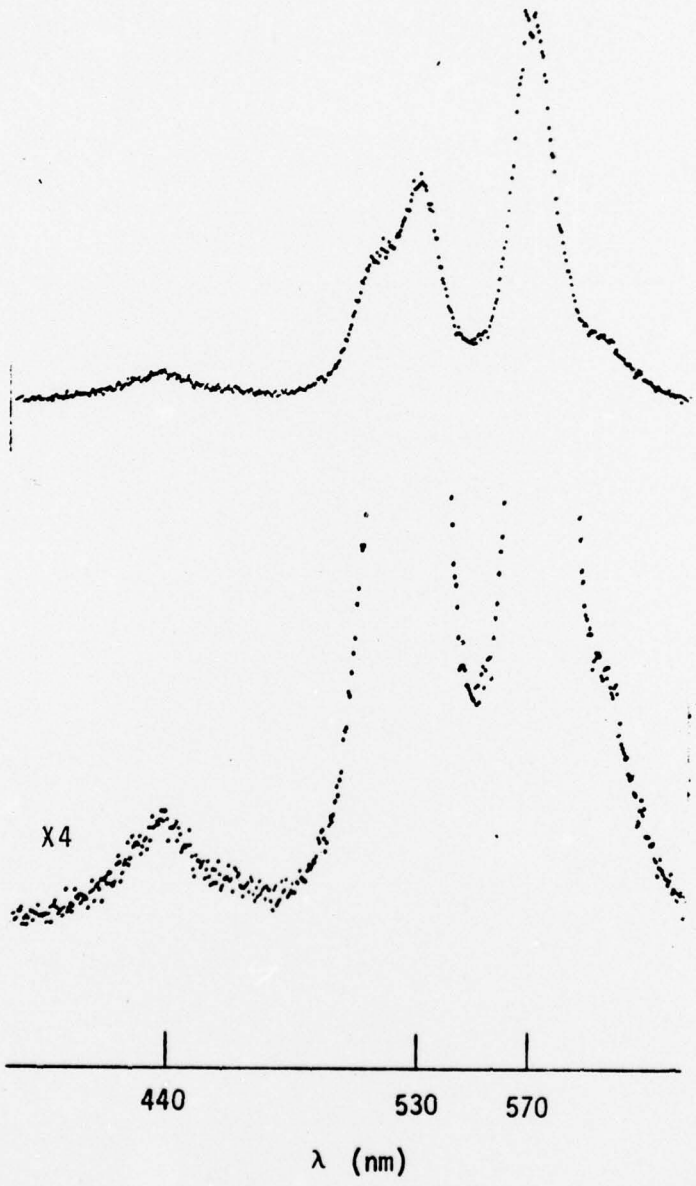
X4
440
530
570
λ (nm)

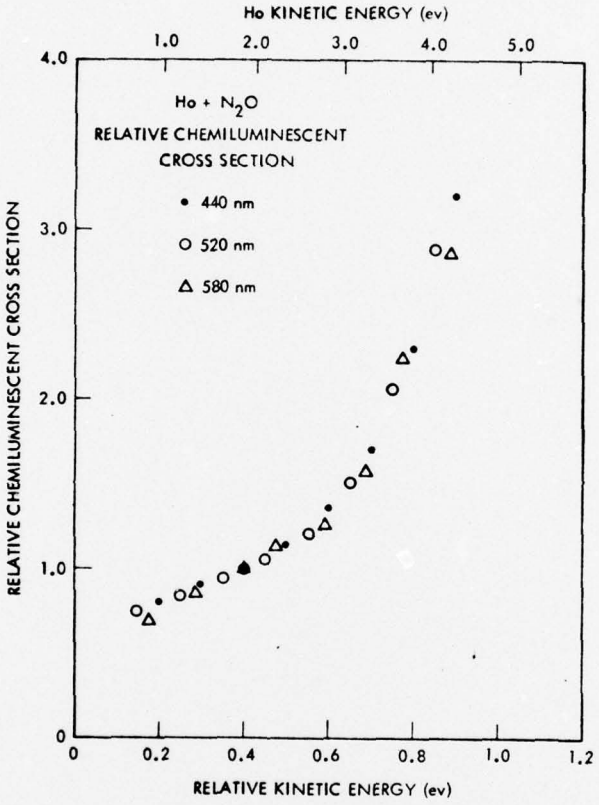
Ho KINETIC ENERGY (ev)
1.0
2.0
3.0
4.0
5.0
Ho + N_2O
RELATIVE CHEMILUMINESCENT
CROSS SECTION
• 440 nm
○ 520 nm
△ 580 nm
RELATIVE CHEMILUMINESCENT CROSS SECTION
4.0
3.0
2.0
1.0
0
0
0.2
0.4
0.6
0.8
1.0
1.2
RELATIVE KINETIC ENERGY (ev)

Appendix C

Paper RC11

Thirty Second Symposium on
Molecular Spectroscopy

The Ohio State University
Columbus, Ohio
June 13-17, 1977

Abstract

"Chemiluminescent Reactions using a New Metal Atom Source"

Brian G. Wicke, S. P. Tang, and J. F. Friichtenicht

The technique of laser vaporization of thin metal films[1] has been adapted for use in studying metal atom plus oxidant chemiluminescent reactions. Most experiments have been performed under single collision conditions in an atomic beam apparatus, although pressures of oxidant up to 100 microns have also been used. Using this metal atom source, techniques have been developed to measure the single collision chemiluminescence spectra in the visible and near ultraviolet, the lifetimes of long-lived (10-100 microseconds) chemiluminescent states, the velocity dependence of the absolute total scattering cross section, the velocity dependence of the chemiluminescent cross section, and (under favorable conditions) the absolute reactive cross section. Prototypical experiments and results will be discussed using N_2O and either Pb or Ho atomic beams, including measurement of the PbO (a) lifetime and observation of a new electronic state in HoO. Some of the results of studies on other metal atom reactions using this versatile atomic beam source will also be discussed briefly.

1. J.F. Friichtenicht, REVIEW OF SCIENTIFIC INSTRUMENTS 45, 51 (1974); S.P.Tang, N.G.Utterback, and J. F. Friichtenicht, JOURNAL OF CHEMICAL PHYSICS 64, 3833 (1976).